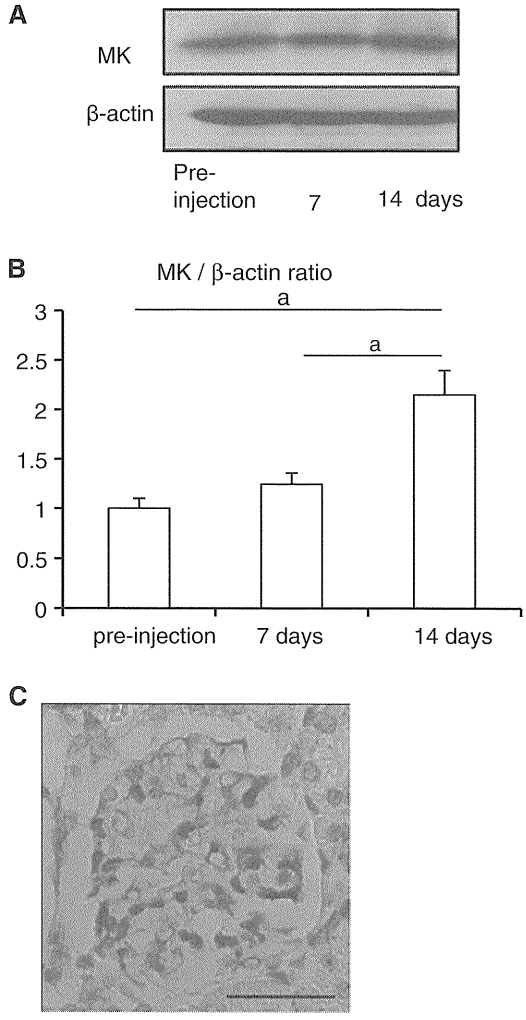

Fig. 5 MK expression in protein-overload $Mdk^{+/+}$ mice. **A** Time course of MK expression, determined by Western blotting. The intensity of MK bands in (**A**) is normalized to that of β-actin (**B**). Data are shown as the mean and SD. *a* $p < 0.01$. $n = 8$ in each group. (**C**) Immunohistochemical staining of MK in glomeruli is shown at 14 days. Scale bar = 50 μm

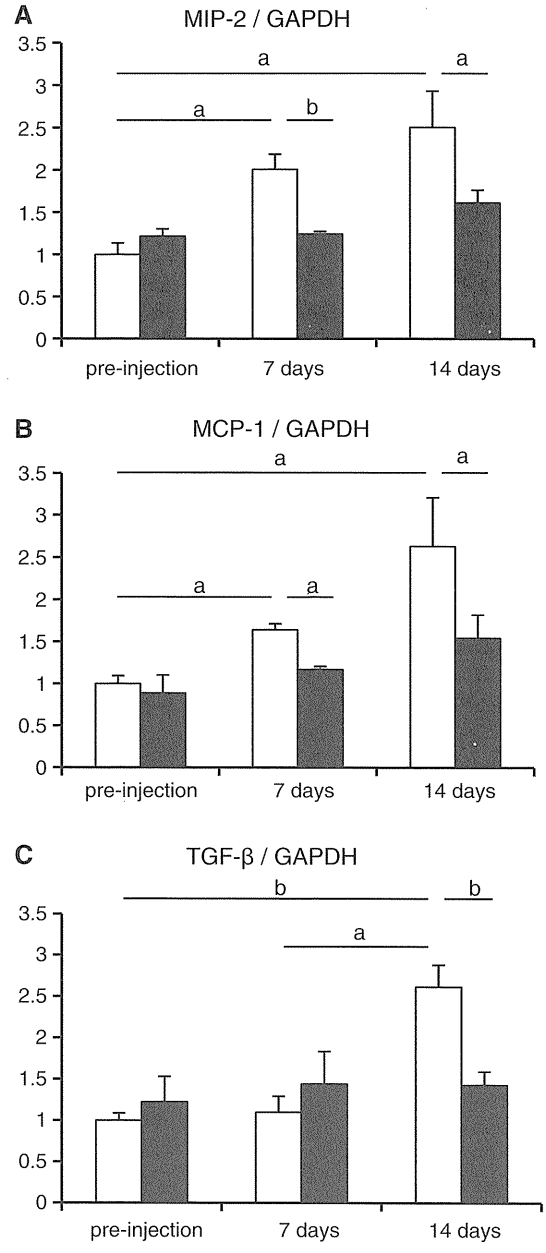

Fig. 6 MIP-2, MCP-1 and TGF-β expression in kidneys of protein-overload $Mdk^{+/+}$ and $Mdk^{-/-}$ mice. Time course of MIP-2 (**A**), MCP-1 (**B**) and TGF-β_1 (**C**) expression, determined by Northern blotting. The intensity of these expressions is normalized to that of GAPDH. Data are shown as the mean and SD. *White columns* $Mdk^{+/+}$ mice; *black columns* $Mdk^{-/-}$ mice. *a* $p < 0.05$, *b* $p < 0.01$. $n = 8$ in each group

Given these findings induced by protein overload, we next addressed the key molecules induced on renal injuries, including MIP-2, MCP-1 and TGF-β_1. MIP-2 and MCP-1 mRNA gradually increased in $Mdk^{+/+}$ mice during the experimental period, whereas the increases were markedly less in $Mdk^{-/-}$ mice (Fig. 6A, B). In addition, TGF-β_1 expression was strikingly enhanced in $Mdk^{+/+}$ mice at 14 days (Fig. 6C).

Discussion

In the present study, we were able to induce endocapillary proliferative glomerulonephritis by protein overload without pre-immunization. In contrast to $Mdk^{-/-}$ mice, $Mdk^{+/+}$ mice demonstrated diffuse cellular proliferation such as mesangial cells and circulating inflammatory cells in the mesangial areas and the capillary lumens, respectively, resulting in both glomerular and tubulointerstitial injuries. These pathological findings could be attributable to neutrophil infiltration through stimulation of the MK–MIP-2 pathway, but appeared to be due to the MK-related IgG deposition and C3 activation.

Most pathological findings due to protein overload were reported in mice as tubulointerstitial injuries. The glomerular lesions are known to be typically mild [11]. The 129/SV mice strain appears to be remarkably susceptible to chronic inflammation-related kidney diseases because of the unique features of their original genetic background [7, 12, 13]. However, Joles et al. [14] documented that routine histology showed no remarkable glomerular injury in both 129/SV and C57BL6/J mice after BSA injections, regardless of the difference of genetic background between these two types of mice. In contrast to previous reports [14, 15], we found that in $Mdk^{+/+}$ mice treated by protein overload, neutrophil infiltration and IgG deposition in glomeruli were increased, resulting in severe endocapillary proliferative glomerulonephritis. Other investigators made a similar rat model, which was treated with lipopolysaccharide (LPS) and BSA overload along with uninephrectomy [16]. BSA (Sigma–Aldrich, cat. number A-4503) used in the first set of experiments had not been processed to reduce endotoxin levels by the manufacturer, and was at least over 200,000 pg/ml. Based on previous reports and our findings, the degree of endocapillary proliferative glomerulonephritis in the 129/SV $Mdk^{+/+}$ mice may depend on both BSA and endotoxin content. We used BSA (Sigma–Aldrich, cat. number A-9430) containing a lower concentration of endotoxin to verify another experiment in vivo. This experimental group did not show glomerular injury in $Mdk^{+/+}$ mice (data not shown). We further examined LPS-induced nephritis in $Mdk^{+/+}$ mice (data not shown); however, this model also exhibited mild glomerular injury and proteinuria, but not severe. These data indicate that these phenomena might be caused by both BSA and the endotoxin content. Our first set of experiments showed characteristics such as reduction of capillary lumen and glomerular hypercellularity due to endogenous glomerular cells and infiltration of neutrophils, and deposition of IgG and complement in the mesangium alongside the basement membrane. These glomerular lesions might be regarded as infection-related glomerular injury in humans.

Our previous studies reported that MK enhanced both neutrophil and macrophage migrations in the tubulointerstitial damage [5, 6, 8]; however, the effect of MK in endocapillary proliferative glomerulonephritis has not yet been identified. Our present study also confirmed the most important role of MK which is to promote infiltration of inflammatory cells directly by its chemotactic activity and indirectly by the induction of MIP-2 in the field of acute glomerulonephritis. Furthermore, Sugiyama et al. [17] documented a cytokine-mediated immune mechanism in a protein-overload mouse model. Complement might also play a pivotal role in the injuries to the glomerular filtration barrier and podocyte [18]. Given these effects, MK may play a new role in stimulating IgG and complement indirectly through cytokine regulation, although we have not evaluated this mechanism completely.

Our current study supports the hypothesis that the existence and induction of MK might be detrimental, especially in a setting in which chemotaxis, inflammatory cytokines and immune complex are severely induced. As expected, the profile of MK expression was strongly consistent with that of glomerular damage and tubulointersitial injury as well as chemokine activation. This study might provide a new insight into understanding the deleterious role of MK in endocapillary proliferative glomerulonephritis, including other renal injuries previously described.

Acknowledgments We thank N. Suzuki, N. Asano and Y. Sawa for excellent technical assistance and H. Aoyama for secretarial assistance.

References

1. Naicker S, Fabian J, Naidoo S, Wadee S, Paget G, Goetsch S. Infection and glomerulonephritis. Semin Immunopathol. 2007;29:397–414.
2. Remuzzi G, Bertani T. Pathophysiology of progressive nephropathies. N Engl J Med. 1998;339:1448–56.
3. Remuzzi G, Ruggenenti P, Benigni A. Understanding the nature of renal disease progression. Kidney Int. 1997;51:2–15.
4. Kadomatsu K, Muramatsu T. Midkine and pleiotrophin in neural development and cancer. Cancer Lett. 2004;204:127–43.
5. Sato W, Kadomatsu K, Yuzawa Y, Muramatsu H, Hotta N, Matsuo S, et al. Midkine is involved in neutrophil infiltration into the tubulointerstitium in ischemic renal injury. J Immunol. 2001;167:3463–9.
6. Kawai H, Sato W, Yuzawa Y, Kosugi T, Matsuo S, Takei Y, et al. Lack of the growth factor midkine enhances survival against cisplatin-induced renal damage. Am J Pathol. 2004;165:1603–12.
7. Kosugi T, Yuzawa Y, Sato W, Kawai H, Matsuo S, Takei Y, et al. Growth factor midkine is involved in the pathogenesis of diabetic nephropathy. Am J Pathol. 2006;168:9–19.
8. Kosugi T, Yuzawa Y, Sato W, Arata-Kawai H, Suzuki N, Kato N, et al. Midkine is involved in tubulointerstitial inflammation associated with diabetic nephropathy. Lab Invest. 2007;87:903–13.
9. Nakamura E, Kadomatsu K, Yuasa S, Muramatsu H, Mamiya T, Nabeshima T, et al. Disruption of the midkine gene (*Mdk*) resulted in altered expression of a calcium binding protein in the hippocampus of infant mice and their abnormal behavior. Genes Cells. 1998;3:811–22.
10. Benigni A, Corna D, Zoja C, Longaretti L, Gagliardini E, Perico N, et al. Targeted deletion of angiotensin II type IA receptor does not protect mice from progressive nephropathy of overload proteinuria. J Am Soc Nephrol. 2004;15:2666–74.
11. Pippin JW, Brinkkoetter PT, Cormack-Abound FC, Durvasula RV, Hauser PV, Kowalewska J, et al. Inducible rodent models of acquired podocyte diseases. Am J Physiol Renal Physiol. 2009;296:F213–29.
12. Ma LJ, Fogo AB. Model of robust induction of glomerulosclerosis in mice: importance of genetic background. Kidney Int. 2003;64:350–5.

13. Hartner A, Cordasic N, Klanke B, Veelken R, Hilgers KF. Strain differences in the development of hypertension and glomerular lesions induced by deoxycorticosterone acetate salt in mice. Nephrol Dial Transplant. 2003;18:1999–2004.
14. Ishola DA, van der Giezen DM, Hahnel B, Goldschmeding R, Kriz W, Koomans HA, et al. In mice, proteinuria and renal inflammatory responses to albumin overload are strain-dependent. Nephrol Dial Transplant. 2006;21:591–7.
15. Eddy AA, Kim H, Lopez-Guisa J, Oda T, Soloway PD, et al. Interstitial fibrosis in mice with overload proteinuria: deficiency of TIMP-1 is not protective. Kidney Int. 2000;58:618–28.
16. Zhang W, Chen X, Shi S, Wei R, Wang J, Yamanaka N, et al. Expression and activation of STAT3 in chronic proliferative immune complex glomerulonephritis and the effect of fosinopril. Nephrol Dial Transplant. 2005;20:892–901.
17. Sugiyama M, Kinoshita K, Kishimoto K, Shimazu H, Nozaki Y, Ikoma S, et al. Deletion of IL-18 receptor ameliorates renal injury in bovine serum albumin-induced glomerulonephritis. Clin Immunol. 2008;128:103–8.
18. Abbate M, Zoja C, Corna D, Rottoli D, Zanchi C, Azzollini N, et al. Complement-mediated dysfunction of glomerular filtration barrier accelerates progressive renal injury. J Am Soc Nephrol. 2008;19:1158–67.

Therapeutic Apheresis and Dialysis

Therapeutic Apheresis and Dialysis 15(4):394–399
doi: 10.1111/j.1744-9987.2011.00964.x

Comparison of Free Light Chain Removal by Four Blood Purification Methods

Kyoko Kanayama,[1] Atsushi Ohashi,[5] Midori Hasegawa,[1] Fumiko Kondo,[4] Yoshihiro Yamamoto,[1] Mayu Sasaki,[1] Hiroki Hayashi,[1] Masao Kato,[4] Ryoko Hattori,[7] Hiroshi Yamashita,[7] Jiro Arai,[6] Junichi Ishii,[3] Nobuhiko Emi,[2] and Yukio Yuzawa[1]

[1]Department of Nephrology, [2]Department of Hematology, [3]Department of Joint Research Laboratory of Clinical Medicine, Fujita Health University School of Medicine, [4]Fujita Health University Hospital, Laboratory of Clinical Medicine, [5]Division of Clinical Engineering Technology, Fujita Health University College, [6]Medical and Biological Laboratories, [7]Toyota Memorial Hospital, Aichi, Japan

Abstract: Renal failure is a frequent complication in patients with multiple myeloma. Immunoglobulin free light chains (FLCs) form casts in the distal tubules, resulting in renal obstruction, and are also directly toxic to proximal renal tubules. Removal of FLCs contributes to renal recovery. High cut-off (HCO) membrane Theralite2100, protein leaking dialyzer PES210Dα, plasma separator Evacure1A20 and β_2 microglobulin adsorption column LixelleS-35 were compared in their FLC removal rate. Dialysis using Theralite2100 or Evacure1A20, diafiltration using PES210Dα and adsorption using LixelleS-35 were performed in an in vitro circuit. The highest removal rate was obtained by Theralite2100 dialysis among the four blood purification methods. Albumin loss was also the greatest in Theralite2100 dialysis. The removal content of FLCs per 1 g albumin loss was better in PES210Dα diafiltration. The removal rate of FLCs by Evacure EC1A-20 dialysis was the third highest. Adsorption of FLCs by the β_2 microglobulin adsorption column Lixelle S-35 was confirmed. In conclusion, Theralite2100 dialysis was the best in removal of FLCs. PES210Dα diafiltration can remove FLCs with smaller loss of albumin. **Key Words:** Blood purification, Free light chain, Multiple myeloma.

Renal failure is a frequent complication in patients with multiple myeloma that causes significant morbidity. In the majority of cases, renal impairment is caused by the accumulation and precipitation of light chains, which form casts in the distal tubules, resulting in renal obstruction. Immunoglobulin free light chains (FLCs) are also directly toxic to proximal renal tubules (1). To date, three randomized controlled trials have evaluated the effectiveness of plasma exchange. Zucchelli et al. (2) concluded that plasma exchange can provide significant benefit in both renal outcome and patient survival. On the contrary, Johnson et al. (3) and Clark et al. (4) concluded that plasma exchange does not provide any significant improvement in either renal outcome or patient survival. Leung et al. (5) performed a retrospective analysis and reported a 75% recovery rate of renal function in patients with FLC reduction over 50% by plasma exchange. Other than plasma exchange, high cut-off (HCO) membranes have been used to remove FLCs in patients with multiple myeloma in Europe (6,7). In countries where HCO membranes are not available, other strategies are needed. We previously reported that hemodiafiltration using protein-leaking dialyzers could become an alternative to plasma exchange as a method of removing FLCs in some patients with myeloma cast nephropathy (8). In the present study, we compared the FLC removal rate of the HCO membrane Theralite2100, protein leaking dialyzer PES210Dα, plasma separator Evacure1A20 and β_2 microglobulin (β_2MG) adsorption column LixelleS-35.

Received December 2010; revised January 2011.
Address correspondence and reprint requests to Dr Midori Hasegawa, Department of Nephrology, Fujita Health University School of Medicine, 1-98 Dengakugakubo Kutukaek-cho, Toyoake, Aichi 470-1192, Japan. Email: mhase@fujita-hu.ac.jp
Presented in part at the 31st Annual Meeting of the Japanese Society for Apheresis held 4–6 November 2010 in Chiba, Japan.

MATERIALS AND METHODS

Study materials

This study was approved by the Ethics Committee of the Fujita Health University School of Medicine, Aichi, Japan. Written informed consent was obtained from the patients. Urine from patients with multiple myeloma was contracted by dialysis using FB-05E (NIPRO Co., Osaka, Japan). The contracted urine was mixed with 1.5 L of plasma obtained from filtrates of plasma exchange. The concentration of FLC was adjusted to similar levels among the patients with multiple myeloma (Table 1).

Extracorporeal renal replacement circuit

Figure 1 shows a diagram of the extracorporeal renal replacement circuit. All experiments were performed for 180 min with a roller blood pump (DBB-72, NIKKISO Co., Tokyo, Japan). The plasma flow rate was set at 120 mL/min and dialysate flow was set at 500 mL/min in all experiments. In diafiltration mode, filtration was done at 50 mL/min. Specimens were obtained from the inlet (C_{Bi}) and outlet (C_{Bo}) of the dialyzer/hemofilter/adsorber and just before the outlet of filtrates (C_F). Acetate-buffered filtration replacement fluids (Sublood A; Fuso Pharmaceutical Industries, Osaka, Japan) were used for diafiltration mode. For filtration, the post-dilution mode was used. Dialysis using Theralite2100 (Gambro Dialysatoren, Hechingen, Germany) or Evacure1A20 (Kawasumi Co., Tokyo, Japan), diafiltration using PES210Dα (NIPRO Co., Osaka, Japan), and adsorption using LixelleS-35(Kaneka Co., Osaka, Japan) were performed. Experiments were performed three times with each membrane.

Measurement of FLCs

The concentration of FLCs was measured using the Freelite Human Kappa Free Kit and Freelite Human Lambda Free Kit (Binding Site, Birmingham, UK).

Calculations

The clearance rate was calculated as follows:

$$\text{Clearance rate (mL/min)} = -\ln[\text{CB(t)}/\text{CB (0)}]\times \text{V/t}$$

where CB(t) is the concentration of FLCs in pooled plasma at t minutes after circulation, CB (0) is the concentration of FLCs in pooled plasma before circulation, and V is the volume of pooled plasma (mL).

The above equation was transformed from a single-compartment model (9):

TABLE 1. *Comparison of free light chain (FLC) removal and loss of albumin*

Model	Surface area (m^2)	Mode	Pre-experimental FLC concentration (mg/L)		Removal rate (%)		Removal contents (mg)		Loss of albumin (g)	Removal contents/ 1 gAlb (mg/g)	
			Kappa	Lambda	Kappa	Lambda	Kappa	Lambda		Kappa	Lambda
Theralite 2100	2.1	Dialysis	4067	1217	96.9	95.3	5667	1620	18	355	101
PES210 Dα	2.1	Diafiltration	3100	1400	86.5	76.1	3775	1394	5	691	260
Evacure 1A20	2.0	Dialysis	4077	1233	59.0	56.3	2975	879	10	388	109
Lixelle S-35	Adsorber volume is 350 mL	Adsorption	2450	1203	49.0	44.0	—	—	—	—	—

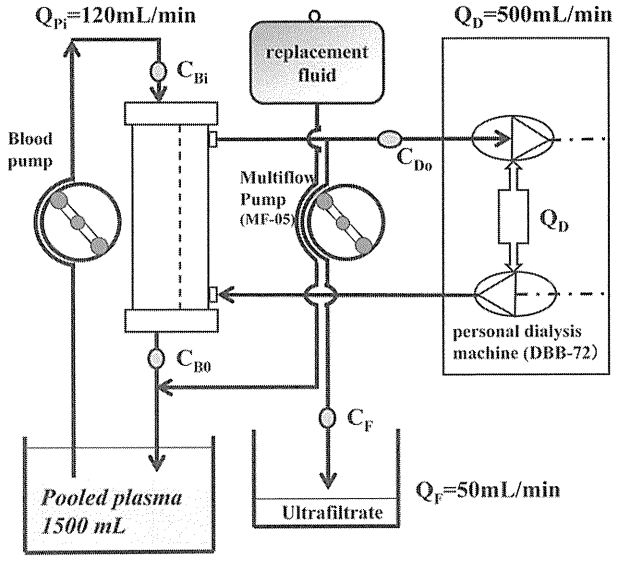

FIG. 1. A diagram of the extracorporeal renal replacement circuit is shown. Specimens were obtained from the inlet (C_{Bi}) and outlet (C_{Bo}) of the dialyzer/hemofilter/adsorber and just before the outlet of filtrates (C_F). Qpi, plasma flow rate; Q_D, dialysis flow rate; Q_F, filtration rate.

$$CB(t) = CB\,(0)\exp(-Kt/V)$$

RESULTS

Table 1 shows the results of FLC removal by the four blood purification methods. The removal rates were 96.9% of kappa FLC and 95.3% of lambda FLC in Theralite2100 dialysis. The highest removal rate was obtained by Theralite2100 dialysis among the four blood purification methods. Albumin loss was the greatest in Theralite2100 dialysis. PES210Dα diafiltration had the second highest FLC removal rate. The removal content of FLC per 1 g albumin loss was the highest in PES210Dα diafiltration. The removal rates were 59.0% of kappa FLC and 56.3% of lambda FLC in Evacure 1A20 dialysis, and 49.0% of kappa FLC and 44.0% of lambda FLC in Lixelle S-35 adsorption. Figure 2 shows the changes in removal rates of FLCs over time. The removal rates increased over time in all four blood purification methods. Figure 3 shows the changes in clearance rate of FLC over time. The clearance rates of Theralite2100 dialysis were the best for both kappa FLC and lambda FLC. The clearance rate decreased over time in Theralite2100 dialysis, PES210Dα diafiltration, and Evacure 1A20 dialysis. The change in clearance rate over time in PES210Dα diafiltration was the largest. In Lixelle S-35adsorption, the change of clearance rate was little over 180 min. Figure 4 shows changes in the albumin concentration over time. In Lixelle S-35adsorption, the albumin concentration did not change after 15 min. There was only a small change in albumin concentration with PES210Dα diafiltration.

DISCUSSION

The highest removal rates of kappa FLC and lambda FLC were obtained by Theralite2100 dialysis among the four blood purification methods. Theralite2100 is a 2.1 m^2 dialyzer with a polyarylethersulfone/polyvinylpyrrolidone membrane and is highly permeable for substances up to 45 kDa. It belongs to the group of HCO membranes. The pore size of HCO membranes is approximately 0.01 μm and, therefore, it is 2- to 3-fold larger than that of conventional high-flux membranes, which have a pore size of 0.003–0.006 μm, and one-twentieth of that of plasma-filtering membranes which have a pore size of around 0.2 μm (10). The in vitro sieving coefficients of the Theralite2100 HCO membrane are as follows: (i) vitamin B12, 1.0; (ii) myoglobin, 0.95; and (iii) albumin, 0.2. The in vitro clearance rate of urea is 199 mL/min, at a Qb of 200 mL/min and a Qd of 500 mL/min. HCO membranes can also remove some humoral mediators of the inflammatory response to sepsis (11).

The clearance of FLCs by PES210Dα diafiltration decreased over time, probably due to fouling. Kappa FLC is a monomer with molecular weight of 22 500 and lambda FLC is a dimer with molecular weight of 45 000. The removal rate and clearance rate of lambda FLC were lower than those of kappa FLC in PES210Dα diafiltration. In Theralite2100 dialysis, the removal rate and clearance rate of kappa FLC and lambda FLC were similar. The amount of albumin loss was 18 g by Theralite2100 dialysis and 5 g by PES210Dα diafiltration. The removal content of FLC per 1 g albumin loss was better in PES210Dα diafiltration. Albumin loss is the main problem of Theralite2100. Lee et al. (12) reported that although removal of β_2MG was superior with HCO membrane than with High-Flux dialysis membranes, serum albumin decreased with the HCO membrane for two weeks. Concerning the effects of albumin leaking, the protein-bound solute is considered to play an essential role in chronic cardiovascular problems (13) or to inhibit endothelial proliferation and wound repair in patients with uremic syndrome (14). The survival benefit of a protein-leaking membrane that removes such protein-bound toxins is controversial (15,16)

The plasma separator Evacure EC1A20 has a sieving coefficient of 0.36 for albumin and can selectively remove low- or intermediate-molecular-weight albumin-bound substances. Other than simple

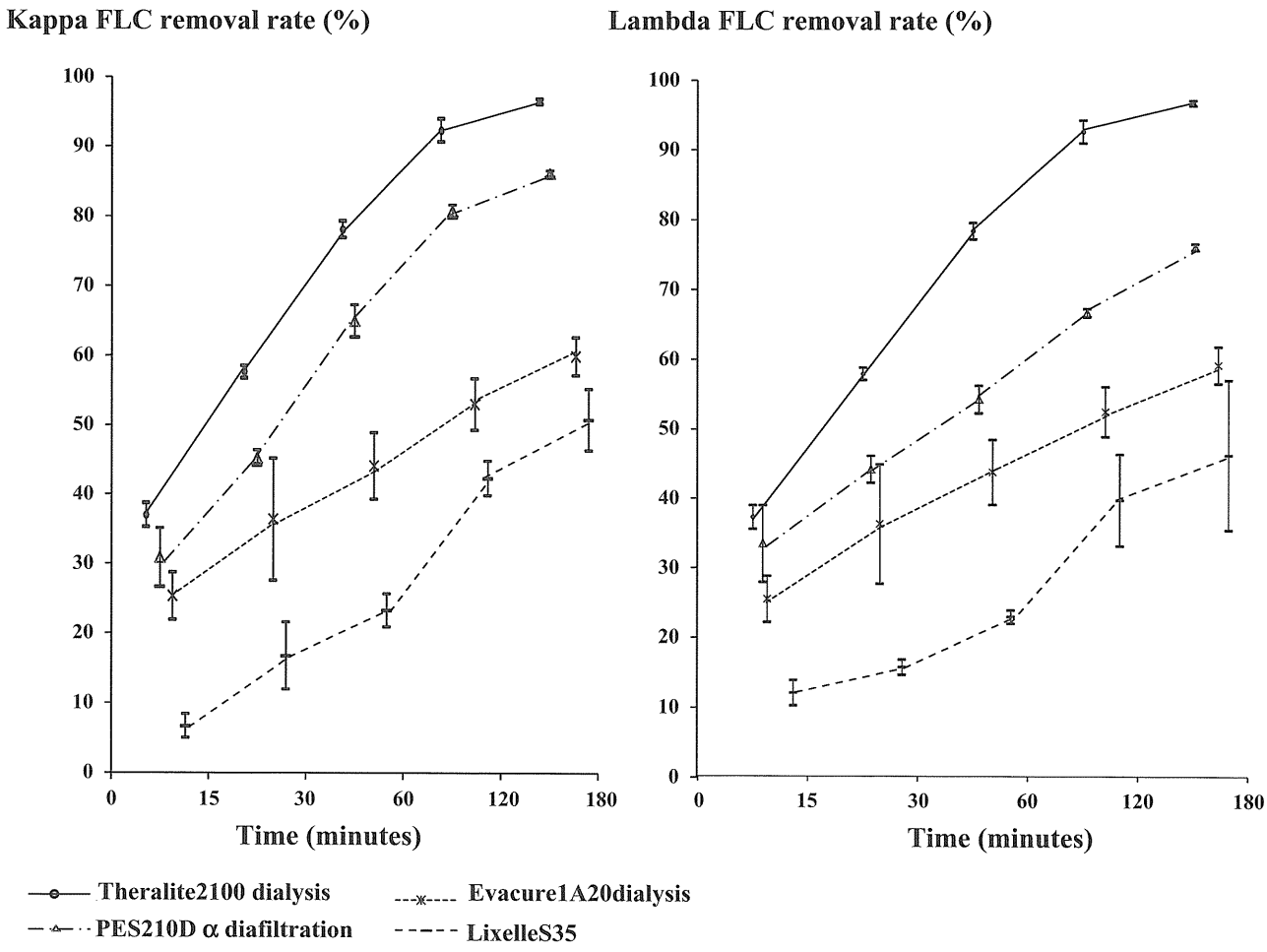

FIG. 2. Changes in the removal rates of kappa free light chain (FLC) and lambda FLC over time with the four blood purification methods. Results are expressed as the mean ± standard deviation ($n = 3$).

plasma exchange, Evacure EC had been reported to be used for selective plasma filtration with dialysis in patients with hepato-renal syndrome (17). In Japan where Theralite2100 is not available, similar characteristics were expected with Evacure EC1A20. Contrary to our expectation, the removal rate of FLC by Evacure EC1A20 dialysis was inferior to that by Theralite2100 dialysis and PES210Dα diafiltration in the 180-min model. There was little change in clearance after 60 min and the removal rate increased over time and, therefore, the removal rate may improve by extending the circuit time.

LixelleS-35 is a β_2 MG adsorption column that consists of porous cellulose beads (18), has a ligand of the hexadecyl group on the surface, and is able to adsorb β_2MG by hydrophobic interaction. It also adsorbs various cytokines (19). In healthy subjects, the concentration of kappa FLC ranges from 3.3 to 19.4 mg/L and that of lambda FLC ranges from 5.7 to 26.3 mg/L. In hemodialysis patients, the concentrations of FLCs are higher than those in healthy subjects and lower than those in patients with multiple myeloma. Hutchison et al. (20) reported that the levels of kappa FLCs were 130 mg/L (53 mg/L to 408 mg/L) and lambda FLCs were 109 mg/L (51 mg/L to 470 mg/L) in hemodialysis patients. FLCs are able to act as uremic toxins by interfering with essential polymorphonuclear leukocyte functions and also attenuate the coordinated apoptotic cell death of neutrophils and therefore may interfere with the normal resolution of inflammation and contribute to the chronic inflammatory state found in patients with deteriorated renal function (21–23). In our study, the removal rates were 49.0% of kappa FLC and 44.0% of lambda FLC over a 180-min period using Lixelle S-35 adsorption. Lixelle S-35 adsorption may also contribute to ameliorating the unfavorable state caused by elevated FLC in patients with dialysis-related amyloidosis.

In this experiment, the plasma flow rate in the extracorporeal renal replacement circuit was set at 120 mL/min. Further experiments are needed to

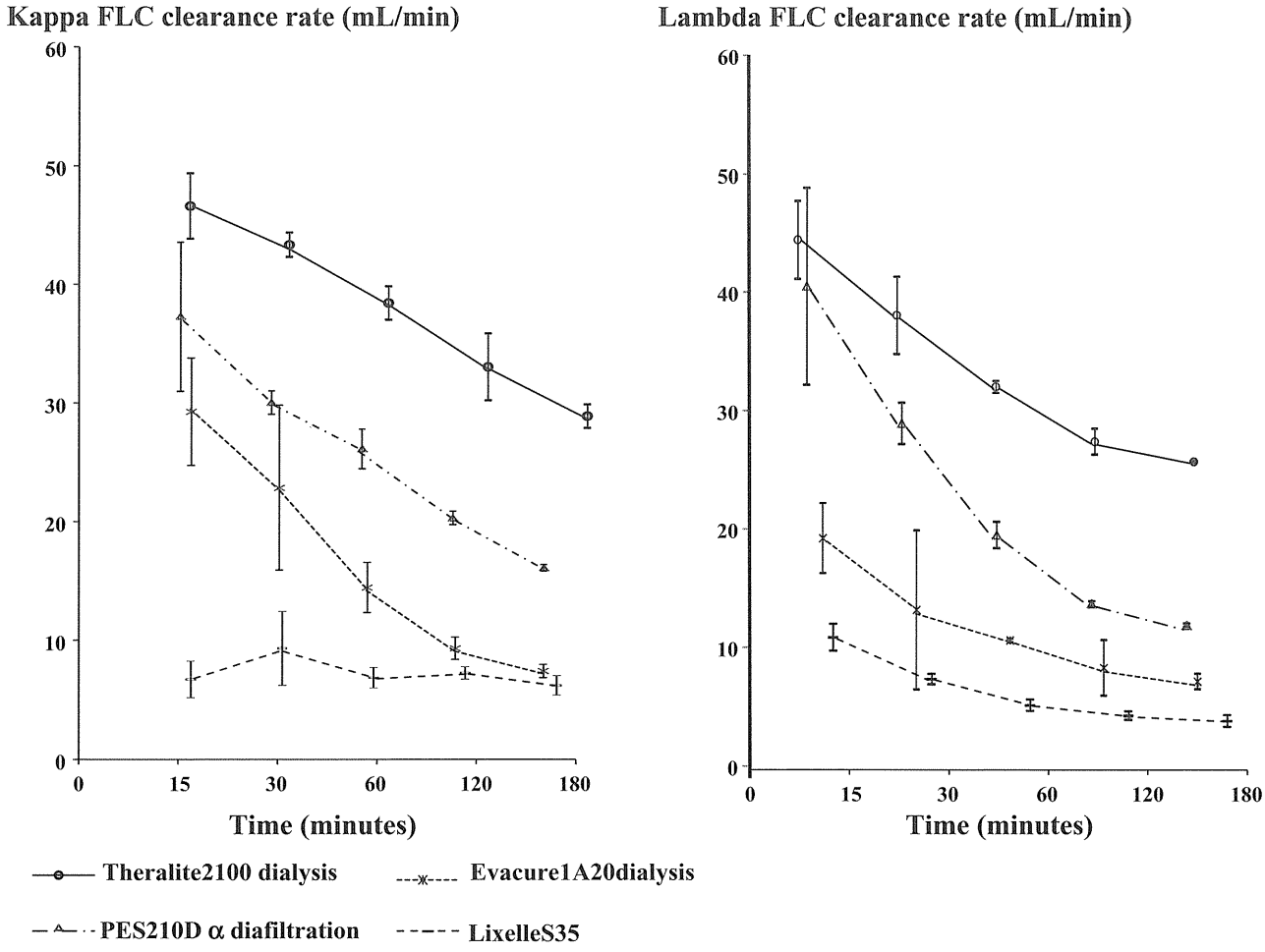

FIG. 3. Changes in the clearance rates of kappa free light chain (FLC) and lambda FLC over time with the four blood purification methods. Results are expressed as the mean ± standard deviation ($n = 3$).

clarify whether the removal rate depends on the plasma flow rate or not.

Hutchison et al. (24) examined four high-flux membranes and two super-flux membranes in vitro. Their initial kappa and lambda FLC contents were each 1000 mg and one liter of serum was recirculated through the dialyzers at 400 mL/min, with transmembrane pressures of between 300 and 400 mm Hg. Their procedure was stopped when production of ultrafiltrate fluid ceased. In their experimental set-up, the reduction rates using APS-1050 (Asahi, Tokyo, Japan) were the highest among the four high-flux membranes (71% of kappa FLC and 65% of lambda FLC were removed). Clinically, the blood flow rate is usually around 200 mL/min and therefore, the reduction rates would be different from their experimental data. BK-F 2.1 was the better of the two super-flux membranes (88% of kappa FLC and 73% of lambda were removed in the Hutchison experiments). In our hospital, when the patient with IgG kappa multiple myeloma whose serum kappa-FLC concentration was 4420 (4230–4610) mg/L underwent 6 h of hemodialysis with a blood flow rate of 200 mL/min using BK-F 2.1, the reduction rate of kappa FLC was 54.7 (38.3–71.0)% (8). In this patient, there was a significant amount of blood residue after each hemodialysis session using the BK-2.1F dialyzer. Because the main removal mechanism of FLC by the BK-2.1F dialyzer is adsorption, clotting of the dialyzer might be inevitable due to the higher serum concentration of FLC.

CONCLUSION

Theralitee2100 dialysis was the best in FLC removal among the four blood purification methods. The removal content of FLC per 1 g albumin loss was better in PES210Dα diafiltration. However, fouling over time is a concern in PES210Dα diafiltration. Evacure EC1A20 dialysis had the third highest FLC removal rate and extending the circuit time might

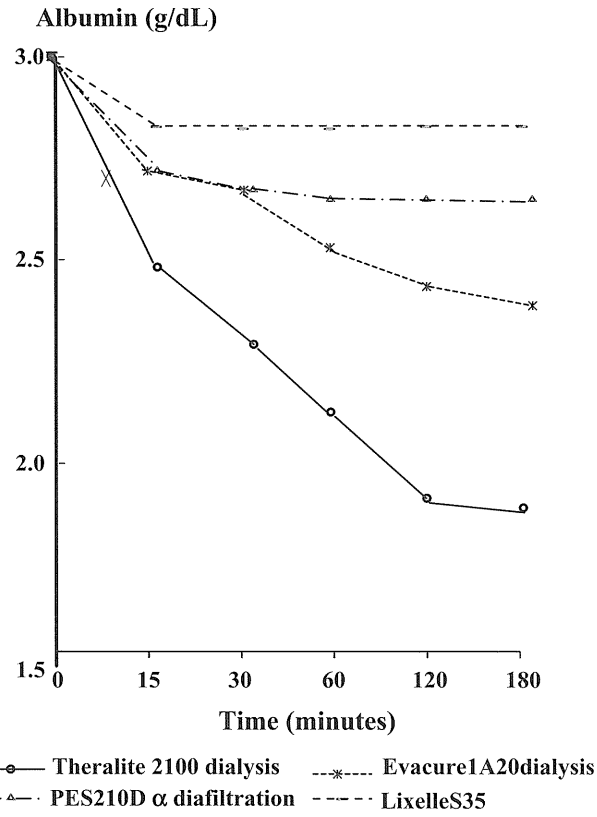

FIG. 4. Changes in the albumin concentration over time with the four blood purification methods. Results are expressed as the mean ($n = 3$).

achieve greater removal. The β_2 MG adsorption column Lixelle S-35 can also contribute to FLC removal as a uremic toxin in hemodialysis patients.

Acknowledgments: We thank Professor Osamu Nishida for his appropriate advice on our experiments.

Conflicts of Interest: None declared.

REFERENCES

1. Dimopoulos MA, Kastritis E, Rosinol L, Bladé J, Ludwig H. Pathogenesis and treatment of renal failure in multiple myeloma. *Leukemia* 2008;22:1485–93.
2. Zucchelli P, Pasquali S, Cagnoli L, Ferrari G. Controlled plasma exchange trial in acute renal failure due to multiple myeloma. *Kidney Int* 1988;33:1175–80.
3. Johnson WJ, Kyle RA, Pineda AA, O'Brien PC, Holley KE. Treatment of renal failure associated with multiple myeloma. Plasmapheresis, hemodialysis, and chemotherapy. *Arch Intern Med* 1990;150:863–9.
4. Clark WF, Stewart AK, Rock GA et al. Canadian Apheresis Group: plasma exchange when myeloma presents as acute renal failure: a randomized, controlled trial. *Ann Intern Med* 2005;143:777–84.
5. Leung N, Gertz MA, Zeldenrust SR et al. Improvement of cast nephropathy with plasma exchange depends on the diagnosis and on reduction of serum free light chains. *Kidney Int* 2008; 73:1282–8.
6. Hutchison CA, Bradwell AR, Cook M et al. Treatment of acute renal failure secondary to multiple myeloma with chemotherapy and extended high cut-off hemodialysis. *Clin J Am Soc Nephrol* 2009;4:745–54.
7. Kleeberg L, Morgera S, Jakob C et al. Novel renal replacement strategies for the elimination of serum free light chains in patients with kappa light chain nephropathy. *Eur J Med Res* 2009;14:47–54.
8. Hasegawa M, Kondo F, Yamamoto K et al. Evaluation of blood purification and bortezomib plus dexamethasone therapy for the treatment of acute renal failure due to myeloma cast nephropathy. *Ther Apher Dial* 2010;14:451–6.
9. Spargen J, Gotch F, Borah M et al. Urea kinetics: a guide to nutritional management of renal failure. *Am J Clin Nutr* 1978; 31:1696–702.
10. Naka T, Haase M, Bellomo R. "Super high-flux" or "high cut-off" hemofiltration and hemodialysis. *Contrib Nephrol* 2010;166:181–9.
11. Morgera S, Haase M, Kuss T et al. Pilot study on the effects of high cutoff hemofiltration on the need for norepinephrine in septic patients with acute renal failure. *Crit Care Med* 2006;34: 2099–104.
12. Lee D, Haase M, Haase-Fielitz A, Paizis K, Goehl H, Bellomo R. A pilot, randomized, double-blind, cross-over study of high cut-off versus high-flux dialysis membranes. *Blood Purif* 2009; 28:365–72.
13. Vanholder R, Van Laecke S, Verbeke F, Glorieux G, Van Biesen W. Uraemic toxins and cardiovascular disease: in vitro research versus clinical outcome studies. *Nephrol Dial Transplant Plus* 2008;1:2–10.
14. Dou L, Bertrand E, Cerini C et al. The uremic solutes p-cresol and indoxyl sulfate inhibit endothelial proliferation and wound repair. *Kidney Int* 2004;65:442–51.
15. Ward RA. Protein-leaking membranes for hemodialysis: a new class of membranes in search of an application? *J Am Soc Nephrol* 2005;16:2421–30.
16. Vanholder R, Glorieux G, Van Biesen W. Advantages of new hemodialysis membranes and equipment. *Nephron Clin Pract* 2010;114:c165–72.
17. Nakae H, Igarashi T, Tajimi K et al. A case report of hepatorenal syndrome treated with plasma diafiltration (selective plasma filtration with dialysis). *Ther Apher Dial* 2007;11:391–39.
18. Nakazawa R, Azuma N, Suzuki M et al. A new treatment for dialysis-related amyloidosis with beta2-microglobulin adsorbent column. *Artif Organs* 1993;16:823–9.
19. Nakatani T, Tsuchida K, Fu O, Sugimura K, Takemoto Y. Effects of direct hemoperfusion with a beta2-microglobulin adsorption column on hypercytokinemia in rats. Y. *Blood Purif* 2003;21:145–51.
20. Hutchison CA, Harding S, Hewins P et al. Quantitative assessment of serum and urinary polyclonal free light chains in patients with chronic kidney disease. *Clin J Am Soc Nephrol* 2008;3:1684–90.
21. Cohen G, Haag-Weber M, Mai B, Deicher R, Hörl WH. Effect of immunoglobulin light chains from hemodialysis and continuous ambulatory peritoneal dialysis patients on polymorphonuclear leukocyte functions. *Am Soc Nephrol* 1995;6: 1592–9.
22. Cohen G. Immunoglobulin light chains in uremia. *Kidney Int* 2003;Suppl 84:S15–S18.
23. Cohen G, Hörl WH. Free immunoglobulin light chains as a risk factor in renal and extrarenal complications. *Semin Dial* 2009; 22:369–72.
24. Hutchison CA, Cockwell P, Reid S et al. Efficient removal of immunoglobulin free light chains by hemodialysis for multiple myeloma: in vitro and in vivo studies. *J Am Soc Nephrol* 2007;18:886–95.

THE JOURNAL OF BIOLOGICAL CHEMISTRY VOL. 286, NO. 37, pp. 32162–32169, September 16, 2011

SOX9 Protein Induces a Chondrogenic Phenotype of Mesangial Cells and Contributes to Advanced Diabetic Nephropathy*[S]

Received for publication, March 28, 2011, and in revised form, July 25, 2011 Published, JBC Papers in Press, July 27, 2011, DOI 10.1074/jbc.M111.244541

Seiji Kishi[‡], Hideharu Abe[‡1], Haruhiko Akiyama[§], Tatsuya Tominaga[‡], Taichi Murakami[‡], Akira Mima[‡], Kojiro Nagai[‡], Fumi Kishi[‡], Motokazu Matsuura[‡], Takeshi Matsubara[¶], Noriyuki Iehara[¶], Otoya Ueda[‖], Naoshi Fukushima[**], Kou-ichi Jishage[‖], and Toshio Doi[‡]

From the [‡]Department of Nephrology, Graduate School of Medicine, Health-Bioscience Institute, University of Tokushima, Tokushima 770-8503, Japan, the Departments of [¶]Orthopedic Surgery and [§]Nephrology, Kyoto University, 54 Kawahara-cho, Shogoin, Sakyo, Kyoto 606-8503, Japan, the [‖]Chugai Research Institute for Medical Science Inc., Shizuoka 412-8513, Japan, and the [**]Chugai Pharmaceutical Co. Ltd., Tokyo 103-0092, Japan

Diabetic nephropathy (DN) is the most important chronic kidney disease. We previously reported that Smad1 transcriptionally regulates the expression of extracellular matrix in DN. Phenotypic change in mesangial cells (MCs) is a key pathologic event in the progression of DN. The aim of this study is to investigate a novel mechanism underlying chondrogenic phenotypic change in MCs that results in the development of DN. MCs showed chondrogenic potential in a micromass culture, and BMP4 induced the expression of chondrocyte markers (SRY-related HMG Box 9 (SOX9) and type II collagen (COL2)). Advanced glycation end products induced the expression of chondrocyte marker proteins downstream from the BMP4-Smad1 signaling pathway in MCs. In addition, hypoxia also induced the expression of BMP4, hypoxia-inducible factor-1α (HIF-1α), and chondrocyte markers. Overexpression of SOX9 caused ectopic expression of proteoglycans and COL2 in MCs. Furthermore, forced expression of Smad1 induced chondrocyte markers as well. Dorsomorphin inhibited these inductions. Glomerular expressions of HIF-1α, BMP4, and chondrocyte markers were observed in diabetic nephropathy mice. These positive stainings were observed in mesangial sclerotic lesions. SOX9 was partially colocalized with HIF-1α and BMP4 in diabetic glomeruli. BMP4 knock-in transgenic mice showed not only similar pathological lesions to DN, but also the induction of chondrocyte markers in the sclerotic lesions. Here we demonstrate that HIF-1α and BMP4 induce SOX9 expression and subsequent chondrogenic phenotype change in DN. The results suggested that the transdifferentiation of MCs into chondrocyte-like cells in chronic hypoxic stress may result in irreversible structural change in DN.

Diabetic nephropathy (DN)[2] is the most common and important chronic kidney disease and is the leading cause of end-stage kidney disease (ESKD) worldwide. The characteristic glomerular changes resulting from DN are thickening of the glomerular basement membrane (GBM) and expansion of the mesangial area caused by increased mesangial extracellular matrix (ECM). Mesangial cells (MCs) are the major source of ECM synthesis in diabetic glomeruli (1–3). Hyperglycemia, advanced glycation end products (AGEs), and transforming growth factor-β (TGF-β) are implicated in the progression of DN by stimulating ECM production in MCs (4–6). In addition, the phenotypic modulation and dedifferentiation of MCs, which are derived from mesenchymal cells, are key pathological events (7, 8). MCs acquired phenotypes not only of activated smooth muscle cells but also of fibroblasts, and subsequently secrete excess ECM proteins.

We previously reported that Smad1 is a direct transcriptional regulator of type IV collagen (COL4), a major component of increased mesangial ECM in DN, as well as other ECM proteins such as type I collagen (COL1), osteopontin, and α-smooth muscle actin (α-SMA) (4, 9). The most critical feature of glomerulosclerosis is mesangial expansion, which is strongly correlated with decreased glomerular filtration rate (GFR) (10). Most importantly, we found that the glomerular expression levels of Smad1 are clearly correlated with the severities of mesangial matrix expansion in rodent DN (9, 11). Therefore, we have concluded that Smad1 plays a central role in the development of DN. However, we still lack mechanistic insight into how Smad1 is involved in phenotypic alteration of MCs and in the irreversible progression of DN. It is generally acknowledged that Smad1 transduces TGF-β signals and also transduces BMP signals through its receptors (12, 13). Although impairment of vascular wall integrity caused by mesangial matrix expansion leads to irreversible glomerulosclerosis, the molecular mechanisms underlying this irreversible change in the phenotypes of MCs in advanced DN are still unknown. We also demonstrated previously that a transcription factor, SRY-related HMG Box 9 (SOX9), is involved in the modulation of transcriptional enhancement of COL4 (14), but we still do not know how this influences the phenotypic alteration of MCs.

It is well recognized that SOX9 is a cartilage-specific transcription factor; that is, the expression of SOX9 is required for

* This research was supported by Grants-in-Aid for Scientific Research of the Japan Society for the Promotion of Science (21591033 and 19590973), Mitsui Sumitomo Welfare Foundation, and The Kidney Foundation, Japan (JKFB09-41).

[S] The on-line version of this article (available at http://www.jbc.org) contains supplemental Fig. S1.

[1] To whom correspondence should be addressed. Tel.: 81-88-633-7184; Fax: 81-88-633-9245; E-mail: abeabe@clin.med.tokushima-u.ac.jp.

[2] The abbreviations used are: DN, diabetic nephropathy; BMP4, bone morphogenetic protein 4; SOX9, SRY-related HMG Box 9; pSOX9, phosphorylated SOX9; COL2, type II collagen; AGEs, advanced glycation end-products; HIF-1α, hypoxia-inducible factor-1α; ESKD, end-stage kidney disease; MCs, mesangial cells; iNOS, inducible nitric-oxide synthase; Tgm, transgenic mice.

the commitment and differentiation of mesenchymal cells toward the chondrogenic lineage in all developing skeletal elements (15). Moreover, SOX9 is responsible for the deposition of ECM, which is composed predominantly of type II collagen (COL2) in chondrocytes (16). Precise regulation of both induction and silencing of SOX9 is required for the normal development of chondrocytes. Conversely, inappropriate or reactivated expression of SOX9 was reported to impair cell phenotype and promote ECM deposition in vascular diseases and fibrosis (17–20). Among the many signaling molecules involved in chondrogenesis, the biological significance of bone morphogenetic proteins (BMPs) has been well established by utilizing pluripotent C3H10T1/2 cells as a model for the initial events of mesenchymal chondrogenesis (21).

We hypothesized that BMP4 and SOX9 would be closely linked to the phenotypic alteration of MCs and to the irreversible progression of diabetic glomerulosclerosis. However, the regulatory mechanism in the interaction between BMP4-Smad1 signaling and SOX9 expression in MCs during the process of diabetic glomerular injuries has not been fully elucidated.

Though hypoxia has been considered a pivotal contributor to tubular atrophy and interstitial fibrosis in the progression of kidney disease (22), recent studies revealed that hypoxia or ischemic stress also affects MCs in various kidney diseases (23–25). Therefore, in addition to hyperglycemia, local hypoxia or ischemic stress and hypoxia-regulated gene expression also could be important factors at the advanced phase of diabetic glomerulosclerosis. A key mediator in cellular responses to hypoxic conditions is hypoxia-inducible factor-1 (HIF-1), a heterodimeric transcription factor consisting of a constitutively expressed β subunit and an O_2-regulated α subunit. A recent report revealed that high glucose also induces HIF-1α expression in MCs (26). Therefore, HIF-1α also could be an important exacerbating factor in the development of glomerulosclerosis. The chondrocyte is a unique cell located at a permanent state of physiological hypoxia, and hypoxia and HIF-1α support cartilaginous matrix accumulation (27, 28) and are permissive factors in chondrocyte differentiation (29, 30). Furthermore, chondrocyte-related main matrix proteins, such as COL2a1 and aggrecan, are not direct targets of HIF but are up-regulated by hypoxia through cartilage-specific transcription factor SOX9 (31).

Based on these findings, we hypothesized that MCs acquire a chondrocyte-like phenotype that SOX9 mediates during glomerulosclerosis progression. We describe here a novel mechanism of chondrogenic phenotype change of MCs in the developing DN.

EXPERIMENTAL PROCEDURES

Cell Culture Experiment—C3H10T1/2 cells were obtained from the American Type Culture Collection. For routine passage, C3H10T1/2 cells were plated as monolayer cultures and maintained in Dulbecco's modified Eagle's medium (DMEM) containing 10% fetal calf serum (FCS) (Invitrogen). A glomerular MC line was established from glomeruli isolated from normal 4-week-old mice (C57BL/6JxSJL/J) and was identified according to a previously described method (32). The MCs were maintained in B medium (a 3:1 mixture of minimal essential medium/F12 modified with trace elements) supplemented with 1 mM glutamine, penicillin at 100 units/ml, streptomycin at 100 mg/ml (Invitrogen), and 10% fetal calf serum (FCS). The cells were plated on 100-mm dishes (Nalge Nunc International, Roskilde, Denmark) and maintained in B medium/10% FCS. Before each assay, the cells were serum starved for 24 h in the medium containing 0.2% FCS. Stimulation with BMP4 (100 ng/ml) (Sigma) was carried out in serum-free culture medium for 24 h. For treatment with dorsomorphin (5 μM), a small-molecule BMP inhibitor (33), dissolved in dimethyl sulfoxide (DMSO) was added to cells 1 h prior to treatment with BMP4 for 24 h. For the hypoxic culture, the cells were cultured at 37 °C with 5% CO_2 and 5% O_2 in a Hypoxia Incubator Chamber (Stemcell Technologies, Vancouver BC, Canada) (34). AGE exposure was performed as previously described (35).

Preparation of AGEs—AGE-BSA was prepared by incubating BSA in phosphate-buffered saline (10 mM, pH 7.4) with 50 mM glucose 6-phosphate for 8 weeks at 37 °C as described previously (36). Unmodified BSA was incubated under the same conditions without glucose 6-phosphate as a control. Protein concentrations were measured by the Bradford method. All AGE-protein-specific fluorescence intensities were measured at a protein concentration of 1 mg/ml. AGE-BSA and control BSA contained 61.3 and 8.31 units of AGE per milligram of protein, respectively.

Chondrogenic Differentiation—To assess the extent of chondrogenesis, micromass cultures of C3H10T1/2 cells or MCs were performed as previously described (37). Cells were trypsinized and resuspended in 10% FCS at a concentration of 10^7cells/ml. A 10-μl drop of cell suspension was placed in the center of a Labtek Permanox chamber slide (Nunc, Naperville, IL). The cells were allowed to adhere for 2–3 h at 37 °C and 5% CO_2, and then 1 ml of F12 medium with or without 100 ng/ml recombinant human BMP4 (Sigma) was added to the culture. The medium was changed every 3 days. Alcian blue staining (pH 1.0) or immunocytochemistry was performed at day 9.

Alcian Blue Staining and Immunocytochemistry—Culture cells were fixed in 4% PFA, washed with water, and stained with Alcian blue 8-GX (Sigma) in 0.1 N HCl for 2 h and then washed twice in 0.1 N HCl to remove nonspecific staining. Immunocytochemistry was performed with anti-SOX9 (Abcam, Cambridge, UK), anti-COL2 antibody (EMD Chemicals, Gibbstown, NJ) after being fixed in 4% PFA followed by incubation with chondroitinase ABC (Seikagaku Biobusiness, Tokyo, Japan). For nuclear staining, DAPI was applied using Cellstain-DAPI solution (Dojindo Molecular Technologies, Kumamoto, Japan). Appropriate fluorescent secondary antibodies were used for visualization, and imaging was done using a fluorescent microscope.

Plasmid Constructs—To construct the expression vector p3xFlag-SOX9, mouse cDNA encoding full-length SOX9 protein was amplified by PCR with Pfu DNA polymerase (Promega, Madison, WI) and subcloned into the p3xFLAG-CMV-7.1 (Sigma). To construct the expression vector pCMV-Myc-Smad1, mouse cDNA encoding full-length Smad1 protein was subcloned into the pCMV-Myc Mammalian Expression Vector (Clontech, Mountain View, CA). The accuracy of the constructs was confirmed by DNA sequencing.

Transient Transfection of MCs—MCs were seeded and grown until 60–80% confluent on 100-mm dishes. The cells were transfected with 0, 1, and 5 μg of expression vector encoding full-length SOX9 or Smad1 by using Fugene6 Transfection Reagent (Roche, Penzberg, Germany) according to the manufacturer's instructions. The cells were harvested in lysis buffer after 24 h incubation, and Western blotting was performed as reported below or trypsinized and resuspended for the micromass culture method.

Western Blotting—Proteins from whole-cell extract or mouse total kidney were separated by 10% SDS-PAGE, transferred onto a nitro-cellulose membrane, and subjected to Western blotting using anti-BMP4 (Santa Cruz Biotechnology), anti-HIF-1α (Novus Biologicals, Littleton, CO), anti-Smad1 (Santa Cruz Biotechnology), anti-phospho-Smad1/5/8, anti-phospho-Smad2, anti-phospho-Smad3 (Cell Signaling Technology, Beverly, MA), anti- type-II collagen (Millipore, Billerica, MA), anti-SOX9 (Millipore), anti-pSOX9 (Abcam), anti-β-actin (Sigma), anti-Flag M2 (Sigma), and anti-Myc (MBL International, Woburn, MA) antibodies. Proteins were visualized using HRP-conjugated secondary antibodies (Dako, Glostrup, Denmark) and ECL detection reagents (GE Healthcare, Milwaukee, WI).

Histological Examination—Light microscopy: Tissue for light microscopy was fixed in methyl Carnoy's solution and embedded in paraffin. Sections (2 μm thick) were stained with periodic acid-Schiff's reagent (PAS) and periodic acid-Schiff methenamine (PASM).

Immunohistochemistry—Kidney sections were processed for immunohistochemistry following standard procedures. To examine the COL4 expression in kidney, ethyl Carnoy's solution-fixed and paraffin-embedded tissue blocks were used. Kidney sections were rehydrated and treated with 0.3% hydrogen peroxide in methanol for 30 min. To eliminate nonspecific staining, sections were incubated with the appropriate preimmune serum for 60 min at room temperature and then incubated with AvidinD and Biotin blocking solutions (Vector Laboratories, Burlingame, CA) for 15 min each. Sections were incubated with anti-COL4 antibody and then incubated with the appropriate biotinylated secondary antibodies followed by incubation with the avidin-biotin peroxidase complex (Vectastain Elite ABC kit, Vector Laboratories). Peroxidase conjugates were subsequently localized using diaminobenzidine tetrahydrochloride. To examine the expression of BMP4, HIF-1α, SOX9, pSOX9, and COL2, an immunofluorescence study was performed using frozen kidney sections. The sections (4-μm thick) were fixed in 4% PFA, blocked with 10% donkey serum, and incubated with anti-BMP4, anti-HIF-1α (Santa Cruz Biotechnology, R&D Systems Minneapolis, MN), anti-SOX9 (Millipore, Santa Cruz Biotechnology), anti-pSOX9 (Abcam) and anti-COL2 (Santa Cruz Biotechnology) antibodies followed by incubation with fluorescent secondary antibody. Staining with DAPI was performed to identify the nuclei of cells.

Animals—All animal experiments were performed in accordance with the Institutional Animal Care and Use Committee of Chugai Pharmaceutical Co. Ltd. and its institutional guidelines. The Review Board of Tokushima University granted ethical permission to undertake this study. The animals were housed under specific pathogen-free conditions at the animal facility of the University of Tokushima.

As a model for advanced DN, transgenic mouse expressing inducible nitric-oxide synthase (iNOS) under control of insulin promoter (iNOS Tgm) was examined in this study. The model showed iNOS expression at the only β cells in pancreas and nitric oxide produced by cytokine-induced iNOS can cause the degeneration of β cells. The destruction of β cells results in a markedly reduced pancreatic islet mass and in the development of type 1 diabetes mellitus. The iNOS Tgm was maintained on CD-1 mouse background (38). No expression of iNOS protein, whose synthesis is directed only in pancreatic islets, was detected in the kidney. Male littermates were screened for the transgenes by PCR amplification and used for analysis. The primers used for the detection of iNOS Tgm were as follows: forward primer, 5′-GTGGGCTATGGGTTTGTGGAAGG-AGA-3′ and reverse primer, 5′-CGATGTCACATGCAGCT-TGT-3′ (39). The iNOS Tgm having blood glucose levels of more than 400 mg/dl were used as diabetic compared with 100–150 mg/dl in control mice. At 48 weeks of age, the mice were killed and analyzed.

To generate tamoxifen-inducible BMP4 transgenic mouse lines, the mutated murine estrogen receptor-Cre (MerCreMer) transgene and the loxP-GFP-loxP-BMP4 transgene under the control of CMV enhanced-β actin promoter of mouse and chicken were used, respectively. For the induction of BMP4 gene expression, 8-week-old double transgenic mice were fed a diet (CE-2, CLEA Japan, Tokyo, Japan) containing 0.02% tamoxifen citrate (Sigma).

RESULTS

Chondrogenic Differentiation of MCs in Response to BMP4 under High Density Micromass Culture Conditions—We first examined the effects of BMP4 in chondrogenic differentiation by using C3H10T1/2 stem cells. These cells were originally isolated from C3H mouse embryos; they behave like mesenchymal stem cells (24) and obtain a chondrocyte phenotype by BMP stimulation in micromass culture systems (40). The formation of chondrogenic nodules in C3H10T1/2 cells treated with BMP4 was confirmed under conditions favorable for chondrogenesis (Fig. 1*A*), indicating that BMP4 acts as an inducer of chondrogenesis. Next, to determine whether or not MCs have chondrogenic potential, we performed a micromass culture method for MCs in the presence or absence of BMP4. The effect of BMP4 on MCs was observed as Alcian blue-positive multicellular nodules similar to those in C3H10T1/2 cells (Fig. 1*B*). COL2, a major chondrocyte-specific component of the cartilage ECM, was induced in BMP4-stimulated MCs (Fig. 1*C*). Moreover, we found that the expression of SOX9 and that of COL2 were significantly induced by BMP4 treatment in the monolayer culture (Fig. 1*D*). From these findings, it is clear that MCs have chondrogenic potential in response to BMP4 *in vitro*.

Diabetic and Hypoxic Conditions Induced Chondrocyte-related Proteins in MCs—Given the evidence that MCs have chondrogenic potential under BMP4 treatment, we examined whether or not diabetic and hypoxic conditions can induce the expression of chondrocytic markers in MCs. Because AGEs have been known as the major factors that contribute to the

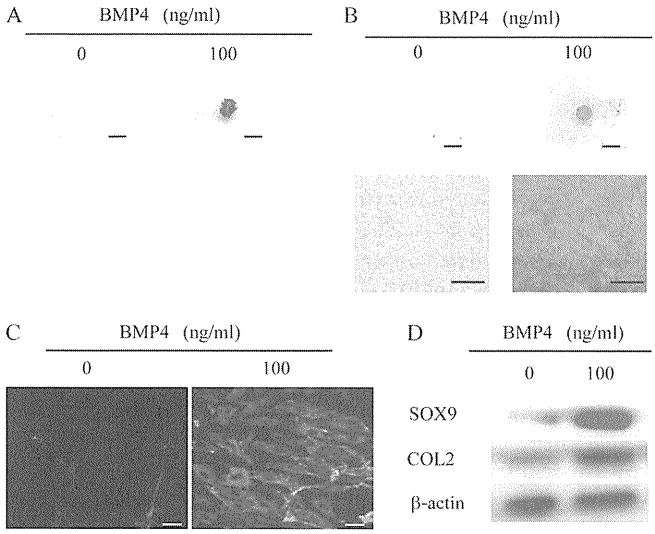

FIGURE 1. **Chondrogenic potential of MCs.** *A*, C3H10T1/2 pluripotent stem cells were cultured under the micromass culture method. Cells were stained with Alcian blue to determine chondrogenesis at day 9 (scale bar, 1 mm). *B* and *C*, MCs were cultured under the micromass culture method. *B*, on day 9, cells were stained with Alcian blue. The *upper panels* are macroscopic findings (scale bar; 1 mm), and the *lower panels* are microscopic findings (original magnification ×400, scale bar; 30 μm). *C*, on day 9, cells were stained with anti-COL2 antibody (original magnification ×400, scale bar; 30 μm). *D*, Western blot analysis of SOX9 and COL2 protein expression in cultured mouse MCs treated with BMP4 for 24 h prior to harvest. β-Actin is the internal control. A representative result is shown from three independent experiments.

pathogenesis of diabetes complications (40), treatment with AGEs was examined in MCs. AGE induced chondrocytic markers (SOX9 and COL2) along with the up-regulation of BMP4 in MCs (Fig. 2*A*). In MCs treated with AGE, Smad2 and Smad3, as well as Smad1, were phosphorylated compared with BSA under exposure to AGE. The treatment with SB431542, a selective inhibitor of TGF-β signaling, and dorsomorphin, a selective small molecule inhibitor of BMP signaling, inhibited the phosphorylation of Smad2/3 and Smad1, respectively (Fig. 2*B*). The increases in SOX9 and COL2 were not inhibited by SB431542 but were inhibited by dorsomorphin (Fig. 2*C*). Next, we investigated whether or not hypoxic stress, which emerges in the advanced stage of DN, affects the chondrocytic change in the MC phenotype. The dramatically increased expression levels of BMP4, HIF-1α, and chondrocytic markers were observed and compared with the control (Fig. 2*D*). These data indicate that diabetic and hypoxic conditions significantly affected the activation of the BMP4-Smad1 signaling pathway and the induction of chondrocyte-related proteins in MCs.

Overexpression of SOX9 Induces Chondrocytic Markers in MCs—To examine whether or not SOX9 has an important role in the induction of chondrogenic phenotype changes in MCs, we carried out an overexpression experiment using a SOX9 expression plasmid. Transient overexpression of SOX9 induced COL2 protein in a dose-dependent manner on monolayer cultures of MCs (Fig. 3*A*). Moreover, the synthesis of proteoglycans was confirmed by Alcian blue staining in a micromass culture of MCs with forced expression of SOX9 (Fig. 3*B*). Double immunofluorescence microscopic analysis revealed that SOX9 was induced mainly in the nucleus and subsequently COL2 was expressed in the cytoplasm of MCs transiently transfected with FLAG-SOX9 (Fig. 3*C*). These findings indicate that MCs are capable of acquiring the chondrocyte phenotype through the induction of SOX9.

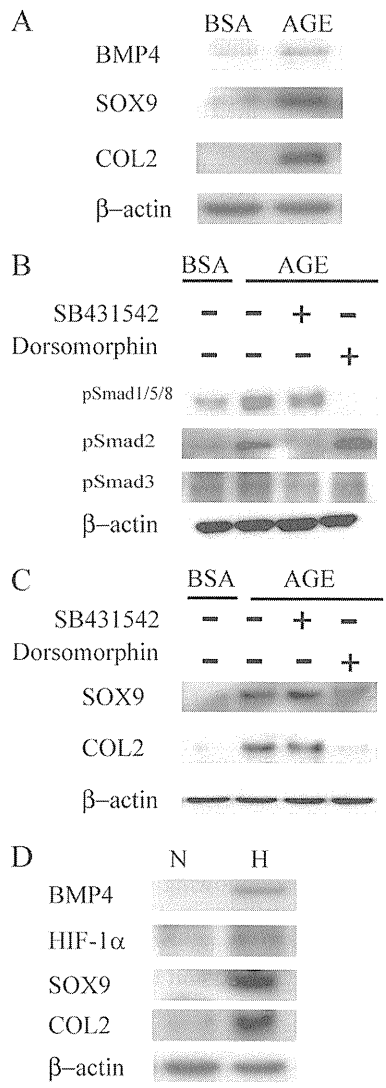

FIGURE 2. **Induction of chondrocyte-related proteins in response to AGEs and hypoxia in mouse MCs.** *A*, cultured MCs were treated with AGEs (5 μg/cm^2) and BSA (5 μg/cm^2) for 48 h. Whole-cell extracts subjected to SDS/PAGE and BMP4, SOX9, and COL2 were detected by Western blotting. *B*, Western blot analysis of pSmad1/5/8, pSmad2, and pSmad3 protein expression in cultured mouse MCs treated with AGEs (5 μg/cm^2) and BSA (5 μg/cm^2) for 6 h prior to harvest. The cells exposed to AGEs were treated with SB431542 or dorsomorphin. *C*, Western blot analysis of BMP4, SOX9, and COL2 protein expression in cultured mouse MCs treated with AGEs (5 μg/cm^2) and BSA (5 μg/cm^2) for 48 h prior to harvest. The cells exposed to AGEs were treated with SB431542 or dorsomorphin. *D*, cultured MCs were treated with normoxia (21% O_2) or hypoxia (5% O_2) for 24 h. Whole-cell extracts were subjected to SDS/PAGE; HIF-1α, BMP4, SOX9, and COL2 were detected by immunoblotting. β-actin is the internal control. *N*, normoxia; *H*, hypoxia. A representative result is shown from three independent experiments.

Smad Signaling Mediates Phenotypic Change in MCs—To investigate the interaction between BMP4-Smad1 signaling and SOX9 expression in MCs, we focused on Smad1, because we previously reported that Smad1 is induced and regulates the expression of other phenotypic markers, such as α-SMA, under diabetic conditions (4). The Smads are intermediates in the BMP signaling pathways of various cell types (41, 42). MCs were

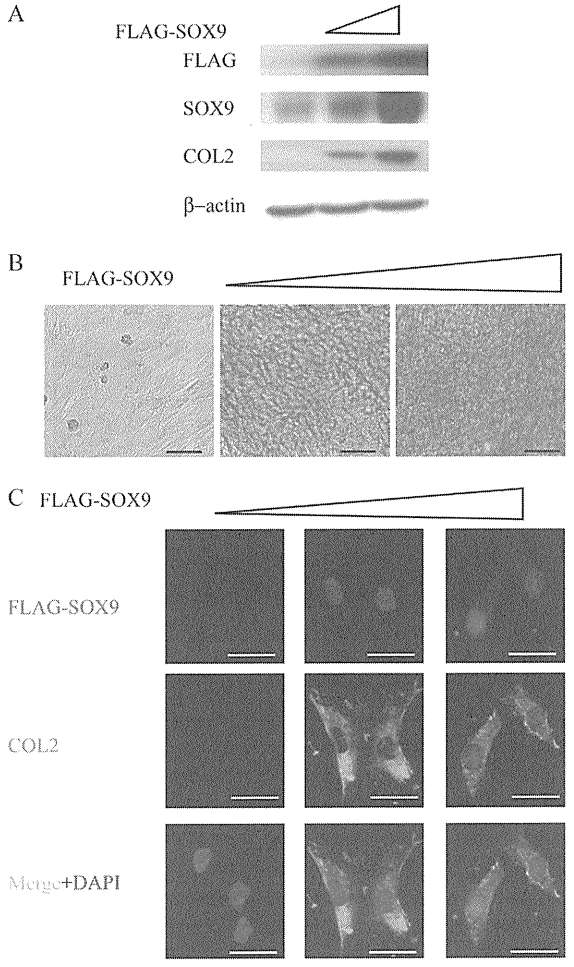

FIGURE 3. **Overexpression of SOX9 induces chondrocytic phenotypic change in the absence of BMP4.** The cells were transfected with full-length SOX9 expression vector (0, 1, and 5 μg plasmid DNA/well) in a dose-dependent manner. *A*, after 24 h cell lysates were prepared, and equal levels of extract protein were separated by SDS/PAGE and immunoblotted with the antibodies indicated. *B*, after 24 h, the cells were trypsinized and cultured under micromass conditions, and on day 3 were stained with Alcian blue (original magnification ×400, scale bar; 30 μm). *C*, after 24 h, the cells were trypsinized and cultured under micromass conditions, and on day 3 were stained with the antibodies indicated (original magnification ×400, scale bar; 30 μm). A representative result is shown from three independent experiments.

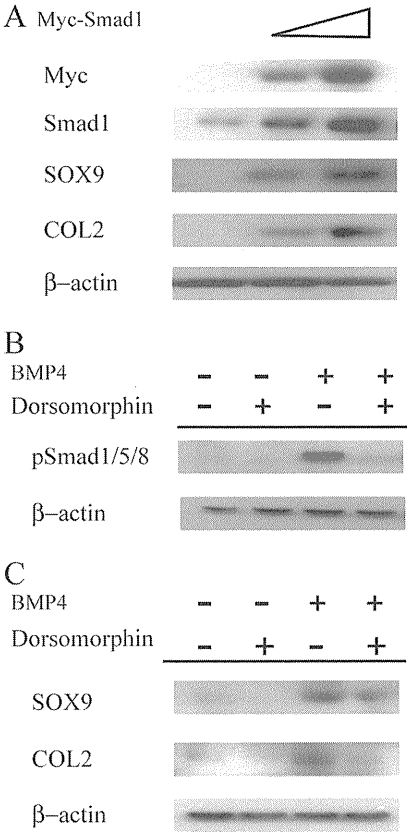

FIGURE 4. **Activation of the BMP4-Smad1 signal pathway causes chondrogenic phenotypic change of MCs.** The cells were transfected with full-length Smad1 expression vector (0, 1, and 5 μg plasmid DNA/well) in a dose-dependent manner. *A*, after 24 h, cell lysates were prepared, and equal levels of extract protein were separated by SDS/PAGE and immunoblotted with the antibodies indicated. *B* and *C*, cells were treated with a specific BMP signaling inhibitor, drosomorphin (10 μM) 1 h before treatment with BMP4 (100 ng/ml). *B*, after 0.5 h cell lysates were prepared, and equal levels of extract protein were separated by SDS/PAGE and immunoblotted with the antibodies indicated. *C*, after 24 h cell lysates were prepared, and equal levels of extract protein were separated by SDS/PAGE and immunoblotted with the antibodies indicated. A representative result is shown from three independent experiments.

either treated with Smad1 expression plasmids to overexpress Smad1 or with 100 ng/ml BMP4 pretreatment with dorsomorphin. Overexpression of Smad1 induced the expression of SOX9 and COL2 in MCs (Fig. 4*A*). Pretreatment with dorsomorphin suppressed the phosphorylation of Smad1/5/8 and diminished the increased expression of SOX9 and COL2 in the presence of *BMP4* (Fig. 4, *B* and *C*). These results provide evidence that Smad1 signaling mediates phenotypic change into chondrocyte-like cells from MCs.

Glomerular Expression of HIF-1α and of Chondrocyte-related Marker in Mice with Diabetic Nephropathy—To further confirm the chondrogenic phenotype change in MCs in diabetes *in vivo*, we examined an experimental advanced diabetic nephropathy model mouse that carries human cDNA for iNOS under the control of the insulin promoter (iNOS Tgm). These mice expressed NOS2 constitutively in pancreatic β cells and developed severe type 1 DM. These mice have been reported to develop severe mesangial matrix expansion and glomerulosclerosis (39) compared with STZ mice and resembled advanced stage of human DN. A marked increase in COL4 expression was observed in iNOS Tgm along with the severe mesangial expansion and glomerulosclerosis (Fig. 5, *A–F*). These histopathological findings importantly resembled those of the irreversible progression of human DN. Furthermore, the iNOS Tgm showed remarkable up-regulation of the expression of BMP4, HIF-1α, SOX9, pSOX9, and COL2 in sclerotic lesions of diabetic glomeruli (Fig. 5, *L–P*). In contrast, the expression of these proteins was nearly absent in normal glomeruli (Fig. 5, *G–K*). In addition, Western blot analyses showed induction of these proteins, corresponding to the histopathological examinations, compared with control mice (Fig. 5*Q*). These data suggest that HIF-1α and chondrocyte-related proteins were induced in advanced damaged glomeruli of DN mice.

Colocalization of HIF-1α, BMP4, and SOX9 in Diabetic Glomeruli—To examine the colocalization of HIF-1α and SOX9, double immunofluorescence staining was carried out.

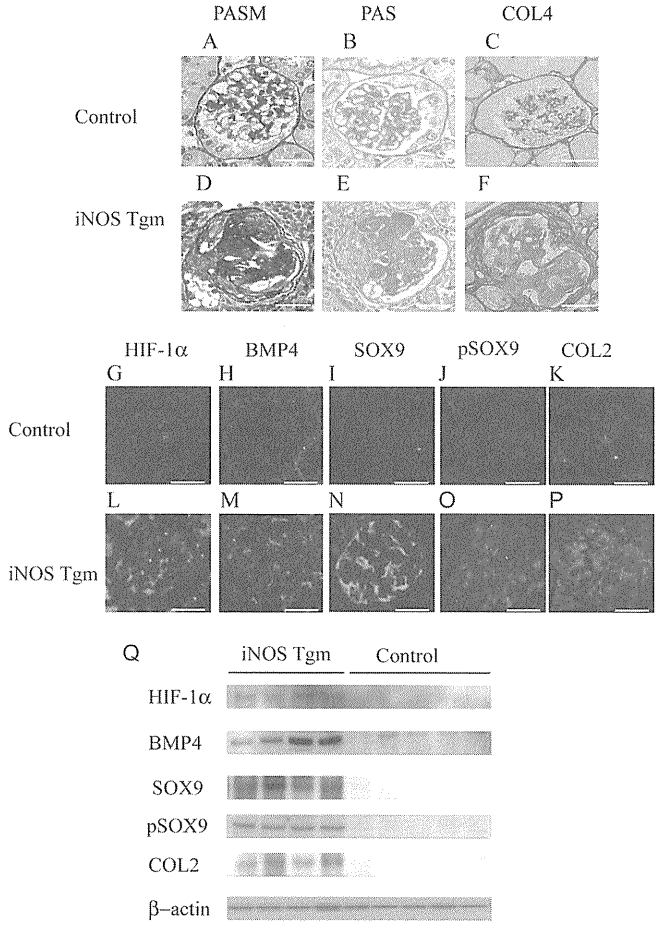

FIGURE 5. **Expressions of HIF-1α, BMP4, SOX9, pSOX9, and COL2 in mouse DN.** *A–F*, representative photomicrographs of periodic acid-Schiff methenamine (PASM), periodic acid-Schiff staining (PAS), and immunohistochemical staining of COL4 are shown (original magnification ×400, scale bar; 30 μm). *G–P*, representative photomicrographs of immunohistochemical staining of HIF-1α, BMP4, SOX9, pSOX9, and COL2 are shown (original magnification ×400, scale bar; 30 μm). The *upper panels* are control mice, and the *bottom panels* are iNOS Tgm at 48 weeks of age. *Q*, Western blots for the whole kidney lysates from each mice are shown ($n = 5$ for control; $n = 4$ for iNOS Tgm). In all, 10 μg of each sample was analyzed with the antibodies indicated. Each lane represents representative data.

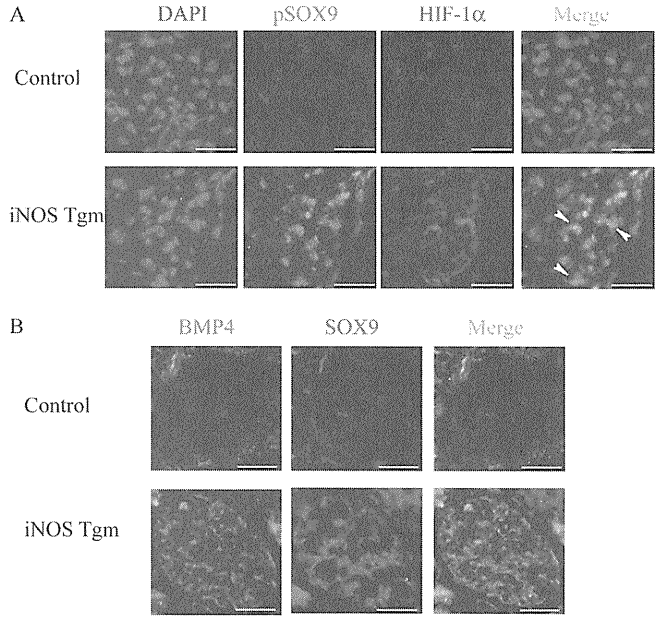

FIGURE 6. **Colocalization of HIF-1α, BMP4, and pSOX9 in mouse DN.** *A*, triple staining of pSOX9 (*green*), HIF-1α (*red*), and DAPI (*blue*) is shown. *Arrowheads* indicate the areas of overlap of HIF-1α and SOX9 in the nuclei. *B*, double staining with BMP4 (*green*) and SOX9 (*red*) is shown. The *upper panels* are control mice, and the *bottom panels* are iNOS Tgm at 48 weeks of age. Original magnification ×400, scale bar; 30 μm.

Coexistence of HIF-1α and an active form of SOX9 (pSOX9) was observed in the nuclei in diabetic glomeruli (Fig. 6*A*). A recent study showed that HIF-1α protein is induced in MCs in a diabetic condition (26). Taken together, these data suggest that these genes expressed in diabetic glomeruli mainly occurred in MCs. Furthermore, SOX9 expression also partially coincided with BMP4 expression in the diabetic glomeruli (Fig. 6*B*).

Evaluation of Chondrogenic Potential in Tamoxifen-inducible BMP4 Transgenic Mice—It is well known that BMP4 is critically involved in the normal embryonic development. We have just recently reported that BMP4 acts as an upstream regulatory molecule for the process of ECM accumulation in DN and provide a new aspect of molecular mechanisms in DN (43). We have developed transgenic mice with inducible expression of BMP4 by using the tamoxifen-regulated Cre/LoxP system. BMP4 transgenic mice (BMP4 Tgm) exhibited pathological features, an expanded mesangial area and a thickened glomerular basement membrane in glomeruli, that remarkably resembles human DN. Tamoxifen-inducible BMP4 Tgm revealed extensive expansion of the mesangial matrix compared with non-transgenic mouse glomeruli (Fig. 7*A* and supplemental Fig. S1). After tamoxifen administration, BMP4 was induced in the areas of GFP disappearance. And these Tgm also showed significant induction of glomerular expression of SOX9 and of COL2 compared with the control mice (Fig. 7*B*). Furthermore, Western blot analyses showed induction of expression of each of these proteins, corresponding to the histological examinations, compared with control mice (Fig. 7*C*). These data suggest that chondrocyte-related proteins were induced by BMP4 *in vivo*.

DISCUSSION

MC, a mesenchymally derived cell, provides structural support to the glomerulus by producing ECM components that form the mesangial matrix (44). Mesenchymal progenitor or stem cells have multipotential differentiation capacity, allowing development along the chondrogenic, osteogenic, myogenic, and adipogenic lineages. In addition, phenotypic change in MCs is an important pathological change in glomerular injury and is the forerunner of glomerulosclerosis. Although many reports have demonstrated that the trans-differentiation of adult MCs to activated myofibroblastic cells is a characteristic change, in this study we showed that MCs have chondrogenic potential under the micromass culture method, thus demonstrating that MCs have chondrogenic potential in DN. This novel potential of trans-differentiation is mediated by the induction of SOX9, a master transcriptional factor of chondrogenesis. Recently, several strands of evidence have implicated unexpected SOX9 expression in diseases such as within the media of calcified vasculature (45), in skin keloid lesions (areas of excessive scarring following trauma) (46), and in liver fibrosis

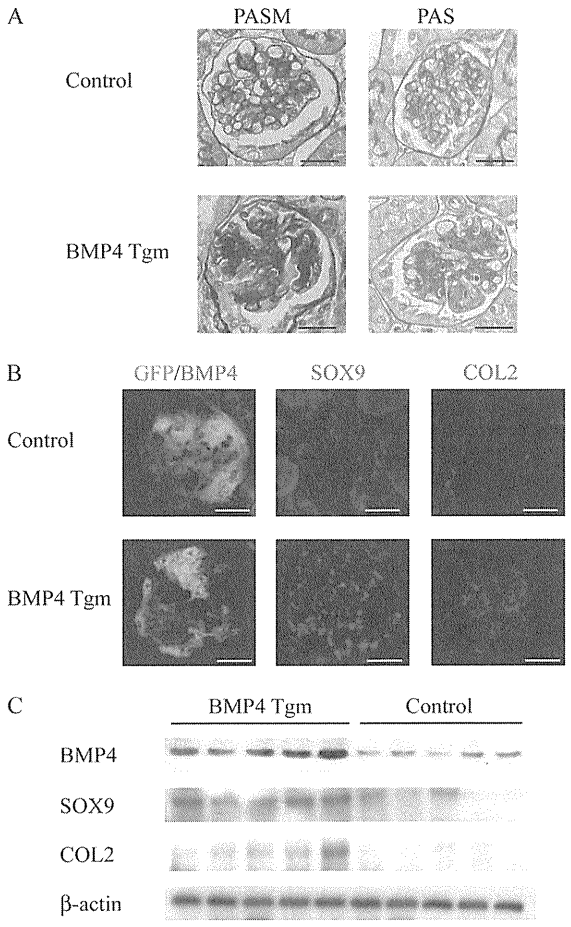

FIGURE 7. **Expression of BMP4, SOX9, and COL2 in sclerotic regions of BMP4 Tgm.** Representative light microscopy (*A*) and immunohistochemistry (*B*) pictures of glomeruli in BMP4 Tgm-treated (BMP4 Tgm) and not treated (Control) with tamoxifen. Original magnification ×400, scale bar; 30 μm. *C*, Western blots for the whole kidney lysates from all mice are shown ($n = 5$ for control; $n = 5$ for BMP4 Tgm). In all, 10 μg of each sample was analyzed with the antibodies indicated. Each lane represents representative data.

(18), causing irreversible changes along with abnormal ECM deposition. Therefore, the acquisition of the chondrocytic phenotype in MCs may be involved in the irreversible changes of diabetic glomerulosclerosis.

In response to a variety of injuries, MCs are generally known to transdifferentiate into myofibroblasts, a specialized population of mesenchymal cells that synthesize an array of different extracellular matrix proteins (*i.e.* type I and type III collagens) that are not normally present in the mesangial matrix and markedly up-regulate the expression of smooth-muscle-like proteins (*i.e.* SMA) (4, 47, 48). We previously demonstrated that Smad1 transcriptionally regulates the expression of SMA and collagens. Moreover, we have shown that SOX9 influences the transcriptional enhancement of COL4 (14), but we still lack mechanistic insight into how SOX9 expression is regulated in DN. Here we have demonstrated that the expression of SOX9 can be induced by BMP4 treatment in MCs. AGE treatment also induced SOX9 expression as well as BMP4 in MCs, suggesting that the BMP4-SOX9 signaling pathway is activated in MCs in diabetes.

The chronic hypoxia conditions of cartilage do not compromise chondrocyte viability, as these cells appear to have developed specific mechanisms to adapt to this environment (49). HIF-1 is a fundamental mediator that is required for the regulation of chondrocyte metabolism. Although hypoxia has been considered a pivotal factor contributing to tubular atrophy and interstitial fibrosis in the progression of kidney disease (23), the role of hypoxia on the progression of irreversible changes in diabetic glomeruli has yet to be determined. In the present study, we have shown that hypoxic stress as well as hyperglycemia induces phenotypic alteration of MCs. In addition to hyperglycemia, hypoxia is thought to be an important microenvironmental factor in the progression of diabetic kidney injury. This trans-differentiation into a chondrogenic phenotype to adapt to chronic hypoxia may be a critical event during the development of glomerulosclerosis. Although HIF-1 is essential for hypoxia-induced angiogenesis in the brain, heart, lungs, or muscle (50), similar adaptive angiogenic responses do not occur in advanced diabetic glomerulosclerosis due to the tuft of glomerular capillary blood vessels located in Bowman's capsule. In general, tissue-level matrix stiffness has a definitive effect on the cell lineage specification (51), and thereby the hypoxia-induced chondrogenic phenotypic change in MCs and subsequent chondrogenic ECM production, which are characteristics of chondrocytes, can be implicated in irreversible glomerular structural changes leading to ESKD because of the up-regulated production of ECM.

The histological hallmark of the DN is mesangial sclerosis, which is characterized by an accumulation of ECM in the mesangial areas, leading to progressive obliteration of the vascular spaces and subsequent ischemic state in its advanced stage. Therefore, we analyzed iNOS Tgm, because they exhibited mesangial expansion and nodular-like lesions resembling an advanced stage of human DN, on the other hand, diabetic models including streptozotocin-induced model show minor glomerular changes. We selected the male heavy proteinuria-positive line from iNOS Tgm. They developed a generalized and diffuse hyperplasia of the mesangial matrix, GBM thickening, and heavy albuminuria. These changes are significantly similar to human DN. The responsible molecule of this established model remains to be elucidated, however, these glomerular lesions were ameliorated by blocking the AGE signaling pathway. These findings suggest iNOS Tgm is an appropriate model for investigating an advanced stage of human DN (39, 52, 53).

In the present study, iNOS Tgm developed severe glomerulosclerosis and showed ectopic induction of BMP4, SOX9, and COL2. In particular, BMP4 is a crucial regulator in the process of chondrogenesis that increases the condensation of limb mesenchyme and directly induces the expression of chondrogenic genes, including SOX9 (54, 55). Furthermore, we very recently revealed that BMP4 plays a central role in the development of DN. BMP4 Tgm showed pathological changes consistent with the features of typical diabetic mesangial matrix hyperplasia and also showed ectopic induction of SOX9 and COL2. As described above, the BMP signal pathway and SOX9 are required for the onset of chondrogenesis, suggesting that BMP4 and SOX9 are candidate regulators of phenotypic change of MC in the advanced stage of DN.

In conclusion, our study suggests that MCs have chondrogenic potential, a new mechanism of impaired differentiation

via the induction of ectopic SOX9. Chondrocytes are the only cells found in cartilage, an avascular and hypoxic mesenchymal tissue (56). Therefore, it makes sense that MCs acquire the chondrogenic phenotype mediated by ectopic SOX9 to operate a cellular-protective mechanism for chronic pathological hypoxic stress in the kidney. BMP4 and HIF-1α, which are known to be upstream molecules of SOX9, have important influences on the phenotypic change of MC into a chondrocyte-like cell in DN. This impaired differentiation mechanism of MCs could be a key event in the development and progression of the irreversible stage of DN.

Acknowledgment—We thank Dr. George W. Meyer (Sacramento Medical Center) for critical reading of the manuscript.

REFERENCES

1. Lenz, O., Striker, L. J., Jacot, T. A., Elliot, S. J., Killen, P. D., and Striker, G. E. (1998) *J. Am. Soc. Nephrol.* **9,** 2040–2047
2. Lupia, E., Elliot, S. J., Lenz, O., Zheng, F., Hattori, M., Striker, G. E., and Striker, L. J. (1999) *Diabetes* **48,** 1638–1644
3. Xia, L., Wang, H., Munk, S., Kwan, J., Goldberg, H. J., Fantus, I. G., and Whiteside, C. I. (2008) *Am. J. Physiol. Renal Physiol.* **295,** F1705–F1714
4. Abe, H., Matsubara, T., Iehara, N., Nagai, K., Takahashi, T., Arai, H., Kita, T., and Doi, T. (2004) *J. Biol. Chem.* **279,** 14201–14206
5. Fornoni, A., Striker, L. J., Zheng, F., and Striker, G. E. (2002) *Diabetes* **51,** 499–505
6. Simonson, M. S. (2007) *Kidney Int.* **71,** 846–854,
7. Makino, H., Kashihara, N., Sugiyama, H., Kanao, K., Sekikawa, T., Shikata, K., Nagai, R., and Ota, Z. (1995) *J. Diabetes Complications* **9,** 282–284
8. Johnson, R. J. (1994) *Kidney Int.* **45,** 1769–1782
9. Matsubara, T., Abe, H., Arai, H., Nagai, K., Mima, A., Kanamori, H., Sumi, E., Takahashi, T., Matsuura, M., Iehara, N., Fukatsu, A., Kita, T., and Doi, T. (2006) *Lab. Invest.* **86,** 357–368
10. Mauer, S. M., Steffes, M. W., Ellis, E. N., Sutherland, D. E., Brown, D. M., and Goetz, F. C. (1984) *J. Clin. Invest.* **74,** 1143–1155
11. Mima, A., Arai, H., Matsubara, T., Abe, H., Nagai, K., Tamura, Y., Torikoshi, K., Araki, M., Kanamori, H., Takahashi, T., Tominaga, T., Matsuura, M., Iehara, N., Fukatsu, A., Kita, T., and Doi, T. (2008) *Diabetes* **57,** 1712–1722
12. Chen, W., Fu, X., and Sheng, Z. (2002) *Chin. Med. J.* **115,** 446–450
13. Massagué, J., Blain, S. W., and Lo, R. S. (2000) *Cell* **103,** 295–309
14. Sumi, E., Iehara, N., Akiyama, H., Matsubara, T., Mima, A., Kanamori, H., Fukatsu, A., Salant, D. J., Kita, T., Arai, H., and Doi, T. (2007) *Am. J. Pathol.* **170,** 1854–1864
15. Akiyama, H., Chaboissier, M. C., Martin, J. F., Schedl, A., and de Crombrugghe, B. (2002) *Genes Dev.* **16,** 2813–2828
16. Bi, W., Deng, J. M., Zhang, Z., Behringer, R. R., and de Crombrugghe, B. (1999) *Nat. Genet.* **22,** 85–89
17. Farrington-Rock, C., Crofts, N. J., Doherty, M. J., Ashton, B. A., Griffin-Jones, C., and Canfield, A. E. (2004) *Circulation* **110,** 2226–2232
18. Hanley, K. P., Oakley, F., Sugden, S., Wilson, D. I., Mann, D. A., and Hanley, N. A. (2008) *J. Biol. Chem.* **283,** 14063–14071
19. Tintut, Y., Alfonso, Z., Saini, T., Radcliff, K., Watson, K., Boström, K., and Demer, L. L. (2003) *Circulation* **108,** 2505–2510
20. Chen, J. H., Yip, C. Y., Sone, E. D., and Simmons, C. A. (2009) *Am. J. Pathol* **174,** 1109–1119
21. Ahrens, M., Ankenbauer, T., Schröder, D., Hollnagel, A., Mayer, H., and Gross, G. (1993) *DNA Cell Biol.* **12,** 871–880
22. Manotham, K., Tanaka, T., Matsumoto, M., Ohse, T., Miyata, T., Inagi, R., Kurokawa, K., Fujita, T., and Nangaku, M. (2004) *J. Am. Soc. Nephrol* **15,** 1277–1288
23. Nishi, H., Inagi, R., Kato, H., Tanemoto, M., Kojima, I., Son, D., Fujita, T., and Nangaku, M. (2008) *J. Am. Soc. Nephrol* **19,** 1500–1508
24. Garin, G., Badid, C., McGregor, B., Vincent, M., Guerret, S., Zibara, K., Hurlstone, A., Laville, M., and McGregor, J. L. (2003) *Am. J. Pathol.* **163,** 2485–2494
25. Neusser, M. A., Lindenmeyer, M. T., Moll, A. G., Segerer, S., Edenhofer, I., Sen, K., Stiehl, D. P., Kretzler, M., Gröne, H. J., Schlöndorff, D., and Cohen, C. D. (2010) *Am. J. Pathol.* **176,** 594–607
26. Xia, L., Wang, H., Munk, S., Frecker, H., Goldberg, H. J., Fantus, I. G., and Whiteside, C. I. (2007) *Am. J. Physiol. Endocrinol. Metab.* **293,** E1280–E1288
27. Pfander, D., Cramer, T., Schipani, E., and Johnson, R. S. (2003) *J. Cell Sci.* **116,** 1819–1826
28. Cramer, T., Schipani, E., Johnson, R. S., Swoboda, B., and Pfander, D. (2004) *Osteoarthritis Cartilage* **12,** 433–439
29. Malladi, P., Xu, Y., Chiou, M., Giaccia, A. J., and Longaker, M. T. (2006) *Am. J. Physiol. Cell Physiol* **290,** C1139–C1146
30. Xu, Y., Malladi, P., Chiou, M., Bekerman, E., Giaccia, A. J., and Longaker, M. T. (2007) *Tissue Eng.* **13,** 2981–2993
31. Amarilio, R., Viukov, S. V., Sharir, A., Eshkar-Oren, I., Johnson, R. S., and Zelzer, E. (2007) *Development* **134,** 3917–3928
32. Davies, M. (1994) *Kidney Int.* **45,** 320–327
33. Yu, P. B., Hong, C. C., Sachidanandan, C., Babitt, J. L., Deng, D. Y., Hoyng, S. A., Lin, H. Y., Bloch, K. D., and Peterson, R. T. (2008) *Nat. Chem. Biol.* **4,** 33–41
34. Hirao, M., Tamai, N., Tsumaki, N., Yoshikawa, H., and Myoui, A. (2006) *J. Biol. Chem.* **281,** 31079–31092
35. Iehara, N., Takeoka, H., Yamada, Y., Kita, T., and Doi, T. (1996) *Kidney Int.* **50,** 1166–1172
36. Doi, T., Vlassara, H., Kirstein, M., Yamada, Y., Striker, G. E., and Striker, L. J. (1992) *Proc. Natl. Acad. Sci. U.S.A.* **89,** 2873–2877
37. Denker, A. E., Haas, A. R., Nicoll, S. B., and Tuan, R. S. (1999) *Differentiation* **64,** 67–76
38. Takamura, T., Kato, I., Kimura, N., Nakazawa, T., Yonekura, H., Takasawa, S., and Okamoto, H. (1998) *J. Biol. Chem.* **273,** 2493–2496
39. Yamamoto, Y., Kato, I., Doi, T., Yonekura, H., Ohashi, S., Takeuchi, M., Watanabe, T., Yamagishi, S., Sakurai, S., Takasawa, S., Okamoto, H., and Yamamoto, H. (2001) *J. Clin. Invest.* **108,** 261–268
40. Vlassara, H., Striker, L. J., Teichberg, S., Fuh, H., Li, Y. M., and Steffes, M. (1994) *Proc. Natl. Acad. Sci. U.S.A.* **91,** 11704–11708
41. Heldin, C. H., Miyazono, K., and ten Dijke, P. (1997) *Nature* **390,** 465–471
42. Massagué, J., and Wotton, D. (2000) *EMBO J.* **19,** 1745–1754
43. Tominaga, T., Abe, H., Ueda, O., Goto, C., Nakahara, K., Murakami, T., Mima, A., Nagai, K., Araoka, T., Kishi, S., Fukushima, N., Jishage, K., and Doi, T. (2011) *J. Biol. Chem.* **286,** 20109–20116
44. Schlondorff, D. (1987) *FASEB J.* **1,** 272–281
45. Neven, E., Dauwe, S., De Broe, M. E., D'Haese, P. C., and Persy, V. (2007) *Kidney Int.* **72,** 574–581
46. Naitoh, M., Kubota, H., Ikeda, M., Tanaka, T., Shirane, H., Suzuki, S., and Nagata, K. (2005) *Genes Cells* **10,** 1081–1091
47. Desmoulière, A., Geinoz, A., Gabbiani, F., and Gabbiani, G. (1993) *J. Cell Biol.* **122,** 103–111
48. Johnson, R. J., Iida, H., Alpers, C. E., Majesky, M. W., Schwartz, S. M., Pritzi, P., Gordon, K., and Gown, A. M. (1991) *J. Clin. Invest.* **87,** 847–858
49. Rajpurohit, R., Koch, C. J., Tao, Z., Teixeira, C. M., and Shapiro, I. M. (1996) *J. Cell. Physiol.* **168,** 424–432
50. Isner, J. M. (2000) *J. Clin. Invest.* **106,** 615–619
51. Engler, A. J., Sen, S., Sweeney, H. L., and Discher, D. E. (2006) *Cell* **126,** 677–689
52. Ohashi, S., Abe, H., Takahashi, T., Yamamoto, Y., Takeuchi, M., Arai, H., Nagata, K., Kita, T., Okamoto, H., Yamamoto, H., and Doi, T. (2004) *J. Biol. Chem.* **279,** 19816–19823
53. Myint, K. M., Yamamoto, Y., Doi, T., Kato, I., Harashima, A., Yonekura, H., Watanabe, T., Shinohara, H., Takeuchi, M., Tsuneyama, K., Hashimoto, N., Asano, M., Takasawa, S., Okamoto, H., and Yamamoto, H. (2006) *Diabetes* **55,** 2510–2522
54. Semba, I., Nonaka, K., Takahashi, I., Takahashi, K., Dashner, R., Shum, L., Nuckolls, G. H., and Slavkin, H. C. (2000) *Dev. Dyn.* **217,** 401–414
55. Zehentner, B. K., Dony, C., and Burtscher, H. (1999) *J. Bone Miner Res.* **14,** 1734–1741
56. Harada, S., and Rodan, G. A. (2003) *Nature* **423,** 349–355

THE JOURNAL OF BIOLOGICAL CHEMISTRY VOL. 286, NO. 22, pp. 20109–20116, June 3, 2011

Activation of Bone Morphogenetic Protein 4 Signaling Leads to Glomerulosclerosis That Mimics Diabetic Nephropathy*

Received for publication, August 30, 2010, and in revised form, March 22, 2011 Published, JBC Papers in Press, April 6, 2011, DOI 10.1074/jbc.M110.179382

Tatsuya Tominaga[‡1,2], **Hideharu Abe**[‡1], **Otoya Ueda**[§], **Chisato Goto**[§], **Kunihiko Nakahara**[¶], **Taichi Murakami**[‡], **Takeshi Matsubara**[**], **Akira Mima**[‡], **Kojiro Nagai**[‡], **Toshikazu Araoka**[‡], **Seiji Kishi**[‡], **Naoshi Fukushima**[‖], **Kou-ichi Jishage**[§], **and Toshio Doi**[‡3]

From the [‡]Department of Nephrology, Graduate School of Medicine, Health-Bioscience Institute, University of Tokushima, Tokushima 770-8503, the [§]Chugai Research Institute for Medical Science Inc., Shizuoka 412-8513, [¶]Hubit Genomix Inc., Tokyo 102-0092, the [‖]Chugai Pharmaceutical Co. Ltd., Tokyo 103-0092, Japan, and the [**]Department of Nephrology, Kyoto University Graduate School of Medicine, Kyoto 606-8507, Japan

Diabetic nephropathy (DN) is the most common cause of chronic kidney disease. We have previously reported that Smad1 transcriptionally regulates the expression of extracellular matrix (ECM) proteins in DN. However, little is known about the regulatory mechanisms that induce and activate Smad1. Here, bone morphogenetic protein 4 (Bmp4) was found to up-regulate the expression of Smad1 in mesangial cells and subsequently to phosphorylate Smad1 downstream of the advanced glycation end product-receptor for advanced glycation end product signaling pathway. Moreover, Bmp4 utilized Alk3 and affected the activation of Smad1 and Col4 expressions in mesangial cells. In the diabetic mouse, Bmp4 was remarkably activated in the glomeruli, and the mesangial area was expanded. To elucidate the direct function of Bmp4 action in the kidneys, we generated transgenic mice inducible for the expression of Bmp4. Tamoxifen treatment dramatically induced the expression of Bmp4, especially in the glomeruli of the mice. Notably, in the nondiabetic condition, the mice exhibited not only an expansion of the mesangial area and thickening of the basement membrane but also remarkable albuminuria, which are consistent with the distinct glomerular injuries in DN. ECM protein overexpression and activation of Smad1 in the glomeruli were also observed in the mice. The mesangial expansion in the mice was significantly correlated with albuminuria. Furthermore, the heterozygous *Bmp4* knock-out mice inhibited the glomerular injuries compared with wild type mice in diabetic conditions. Here, we show that BMP4 may act as an upstream regulatory molecule for the process of ECM accumulation in DN and thereby reveals a new aspect of the molecular mechanisms involved in DN.

Diabetic nephropathy (DN)[4] is the most common cause of chronic kidney disease and end-stage renal disease in the world. DN is characterized by mesangial matrix expansion caused by an excessive deposition of extracellular matrix (ECM) proteins in the mesangial area, which ultimately progresses to glomerulosclerosis associated with renal dysfunction (1, 2). Advanced glycation end products (AGE) produced as the result of hyperglycemia are known to stimulate the production of ECM proteins, resulting in glomerulosclerosis (3–5). One of the major components of ECM is $\alpha1/\alpha2$ type IV collagen (Col4), which is overproduced in diabetic glomerulosclerosis. We have previously demonstrated that Smad1 directly binds to the promoter of Col4 and transcriptionally up-regulates Col4 expression (6). In addition, glomerular expression of Smad1 is significantly increased in diabetic rats along with mesangial expansion (7, 8). In previous reports, it has been shown that Smad1 is absent in the renal glomeruli of normal adult human and mice (6). For now, we still lack mechanistic insight into how Smad1 expression is induced and activated in DN. It is generally known that Smad1 is directly phosphorylated by TGF-β type I receptors as well as bone morphogenetic proteins (BMPs) through type I and II BMP receptors (9). Although BMPs are well known to be required for the normal development of various tissues and organs, including the kidneys (10), the role of BMPs in adults or in diseases is unclear. Moreover, the underlying molecular mechanisms of the BMP signaling pathway involved in the pathogenesis of DN remain largely unknown.

Previous studies have reported that TGF-β and its downstream signaling are critical factors in mediating mesangial cell hypertrophy and fibronectin synthesis in diabetes and that angiotensin II plays an important role in the development of mesangial matrix expansion (11, 12). Angiotensin II type 1 receptor blocker (AT1 antagonist) or an angiotensin-converting enzyme inhibitor has been proved to slow slightly the progression of DN (13, 14). However, medical research has still not found a way to halt the progression of DN. From these facts, we hypothesized that there might be other signaling pathways contributing to the progression of DN. Therefore, in this study we tried to dem-

* This work was supported by Grants-in-aid for Scientific Research of the Japan Society for the Promotion of Science 21591033, 19590973, and 22390169, Japan Science and Technology Agency Grant AS2115050G, the Mitsui Sumitomo Welfare Foundation, and The Kidney Foundation of Japan Grant JKFB09-41.

[1] Both authors contributed equally to this work.

[2] Present address: Dept. of Biomedical Laboratory Sciences, Health Sciences, Graduate School of Medicine, Health-Bioscience Institute, University of Tokushima, 3-18-15 Kuramoto-cho, Tokushima-city, Tokushima, 770-8503, Japan. Tel.: 81-88-633-7184; Fax: 81-88-633-9245.

[3] To whom correspondence should be addressed. E-mail: doi@clin.med.tokushima-u.ac.jp.

[4] The abbreviations used are: DN, diabetic nephropathy; MCM, MerCreMer; MC, mesangial cell; ECM, extracellular matrix; AGE, advanced glycation end product; RAGE, receptor for advanced glycation end product; BMP, bone morphogenetic protein; STZ, streptozotocin; tgm, transgenic mice; GBM, glomerular basement membrane.

onstrate that the BMP signaling pathway is a regulatory molecular mechanism directly involved in the pathological features in DN by using both *in vitro* and *in vivo*. We generated inducible *Bmp4* transgenic mice (tgm) by using the tamoxifen-regulated Cre-loxP system and provided an ideal model to investigate the direct role of Bmp4 in glomerular injury *in vivo*.

EXPERIMENTAL PROCEDURES

Experimental Animals—All animal experiments were performed in accordance with Institutional Animal Care and Use Committee of Chugai Pharmaceutical Co. Ltd. and Institutional guidelines, and the ethical Review Board of Tokushima University granted permission for the procedures used in this study.

To generate inducible *Bmp4* transgenic mouse lines, we used the tamoxifen-regulated Cre-loxP system. This system consists of two transgenes. The first transgene is the inducible *Bmp4* expression cassette, *pMacII*-floxed *GFP pA-Bmp4*, by using expression vector pMacII, consisting of cytomegalovirus enhancer, mouse β-actin promoter, and mouse β-globin genomic DNA (Fig. 4*A*, *panel a*). The second transgene is a construct for expression of a fusion protein of mutated murine estrogen receptor and Cre recombinase (MerCreMer (MCM)) with the pCAGGS vector (Fig. 4*A*, *panel b*) (15). *MCM* cDNA was a kind gift from Prof. M. Reth (16). Each of these two transgenes was microinjected to the pronuclei of C57BL/6J mouse fertilized eggs to make transgenic mouse lines. Two strains of inducible *Bmp4* transgenic mouse lines were established as double transgenic mice, C57BL/6J-Tg(Actb-GFP-Bmp4)1Csk-Tg (CAG-MerCreMer)67Csk and C57BL/6J-Tg(Actb-GFP-Bmp4)5Csk-Tg(CAG-MerCreMer)67Csk. In this system, Cre is expressed and remains in the cytoplasm of expressing cells, where it is in an inactive form bound to heat shock protein 90 (Hsp90). After injection of tamoxifen, Cre is released from the Hsp90 and translocates to the nucleus, where it becomes active and mediates recombination of DNA-carrying loxP target sequences. MerCreMer contains two mutated estrogen receptor-binding domains and confers tight dependence on tamoxifen binding for translocation to the nucleus and recombinase activity (17, 18). To induce *Bmp4* gene expression, 8-week-old transgenic mice were fed a diet (CE-2, CLEA, Japan) containing 0.02% tamoxifen citrate (Sigma).

Eight-week-old male C57BL/6 mice weighing 22–24 g were rendered diabetic by the intraperitoneal injection of 50 mg per kg body weight streptozotocin (STZ) in citrate buffer, pH 4.5, for 5 consecutive days. The diabetic state was confirmed 5 days after final injection by measurement of blood glucose level. All mice that were given STZ had a blood glucose concentration exceeding 400 mg/dl and were considered diabetic.

Bmp4 knock-out mice (C57BL/6 $Bmp4^{+/-}$) were gifts of B. Hogan and M. Saitou. Generation and characterization of this mutant mouse were described elsewhere (19). $Bmp4^{+/-}$ mice were maintained on a C57BL/6 background. Diabetes was induced in 8-week-old male mice weighing 22–24 g by the intraperitoneal injection of 100 mg per kg of body weight STZ in citrate buffer, pH 4.5, for 2 days. Mice receiving an injection of citrate buffer were used as controls. The levels of blood glucose were determined 1 week after final injection of STZ. The mice that were given STZ with blood glucose levels exceeding 400 mg/dl were considered diabetic. The mice were classified into four groups as follows: (*a*) nondiabetic C57BL/6 ($n = 6$); (*b*) nondiabetic $Bmp4^{+/-}$ ($n = 6$); (*c*) diabetic C57BL/6 ($n = 8$); and (*d*) diabetic $Bmp4^{+/-}$ ($n = 7$). These mice were killed 20 weeks after final injection of STZ and citrate buffer.

Cell Culture Experiment—A glomerular mesangial cell line was established from glomeruli isolated from normal 4-week-old mice (C57BL/6) and identified according to a method described previously (20). Phenotypically stable cells, passage 14–24, were plated in 100-mm plastic dishes (Nunc) and maintained in B medium (a 3:1 mixture of minimal essential medium/F-12 modified with trace elements) (Nissui) supplemented with 1 mM glutamine, penicillin at 100 units/ml, streptomycin at 100 mg/ml (Invitrogen), and 20% fetal calf serum (FCS) (Invitrogen). The cultured cells fulfilled the criteria generally accepted for glomerular mesangial cells (20).

AGE-BSA was prepared by incubating BSA (fraction V) in phosphate-buffered saline (10 mM, pH 7.4) with 50 mM D-glyceraldehyde for 7 days at 37 °C with protease inhibitors and antibiotics as described previously (3, 21). Unmodified BSA was incubated under the same conditions without D-glyceraldehyde as a control. Preparations were tested for endotoxin, but endotoxin was not detected. Protein concentrations were measured by the Bradford method. All AGE protein-specific fluorescence intensities were measured at a protein concentration of 1 mg/ml. AGE-BSA contained 59.4 AGE units/mg of protein, and unmodified BSA contained 2.3 AGE units/mg of protein, respectively. The glomerular mesangial culture was examined with AGE exposure as described previously (4). These cells were seeded on 100-mm plastic dishes and maintained in B medium/10% FCS. After a 48-h incubation, cells were starved for 24 h in Opti-MEM (Invitrogen) and then incubated with Bmp4 (R&D Systems) at 37 °C for the indicated times. These cells were incubated with carboxymethyl lysine (Nippi) at 10 μg/ml for 24 h followed by serum starvation.

For the receptor for AGE (RAGE) and *Bmp4* knockdown experiments, the cells were analyzed 48 h post-transfection with siRNA for *RAGE* or scrambled siRNA (Invitrogen) and siRNA for *Bmp4* or scrambled siRNA (TAKARA). *Alk3* knockdown experiments were performed by transfecting the cells with shRNA for *Alk3* or control (Takara), followed by serum starvation and stimulation with Bmp4 after 24 h.

Western Blotting—Western blots were performed with anti-Bmp4 (Santa Cruz Biotechnology), anti-Smad1 (Sp125, a mouse monoclonal antibody specific for Smad1, was generated in this study), anti-phospho-Smad1/5/8 (Cell Signaling), anti-Col4 (Southern Biotech), anti-RAGE (ABR), anti-Alk3 (Abgent), anti-β-actin (Sigma), and anti-α-tubulin (Sigma) antibodies.

Histological Examination—Tissue for light microscopy was fixed in methyl Carnoy's solution and embedded in paraffin. Sections were stained with periodic acid Schiff and periodic acid methenamine silver-stained. Morphometry was evaluated in periodic acid methenamine-stained tissues by image processor for analytical pathology as described previously (22). Kidney sections were treated with anti-Bmp4, anti-phospho-Smad1 (Upstate), anti-Smad1, anti-Col4, and Col1 (Abcam) antibod-

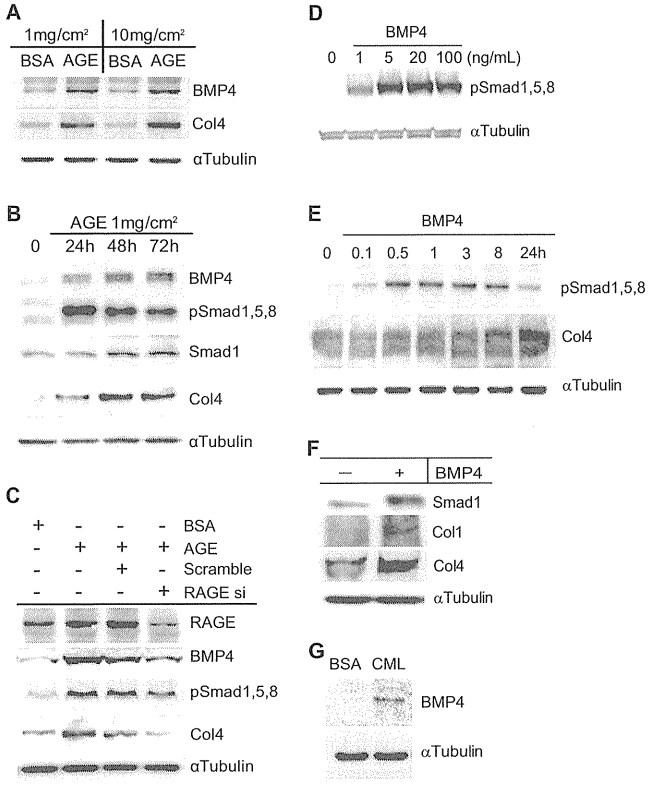

FIGURE 1. **AGE and *Bmp4* showed increased ECM proteins in mouse mesangial cells.** *A*, expression of Bmp4 and Col4 detected by immunoblot after treatment with AGE (1 or 10 $\mu g/cm^2$) and BSA (1 or 10 $\mu g/cm^2$) for 48 h. Equivalent protein loading was confirmed by α-tubulin. Specific proteins were detected by Bmp4 and Col4. *B*, expression of Bmp4, pSmad1/5/8, Smad1, and Col4 after stimulation by AGE 1 $\mu g/cm^2$ for the indicated times by immunoblot. *C*, expression of RAGE, Bmp4, and Col4 after treatment with AGE detected by immunoblot with RAGE siRNA (*siRAGE*) or scrambled siRNA (*scramble*) for 48 h. *D*, phosphorylation of Smad1/5/8 after stimulation by Bmp4 (1–100 ng/ml) for 30 min detected by immunoblot. *E*, phosphorylation of Smad1/5/8 and expressions of Col4 after stimulation by Bmp4 (20 ng/ml) for 0.1–24 h detected by immunoblot. *F*, expression of Smad1 and Col1 after stimulation by Bmp4 (20 ng/ml) for 24 h detected by immunoblot. *G*, expression of Bmp4 detected by immunoblot after treatment with CML (10 $\mu g/ml$). The data are representative of three independent experiments.

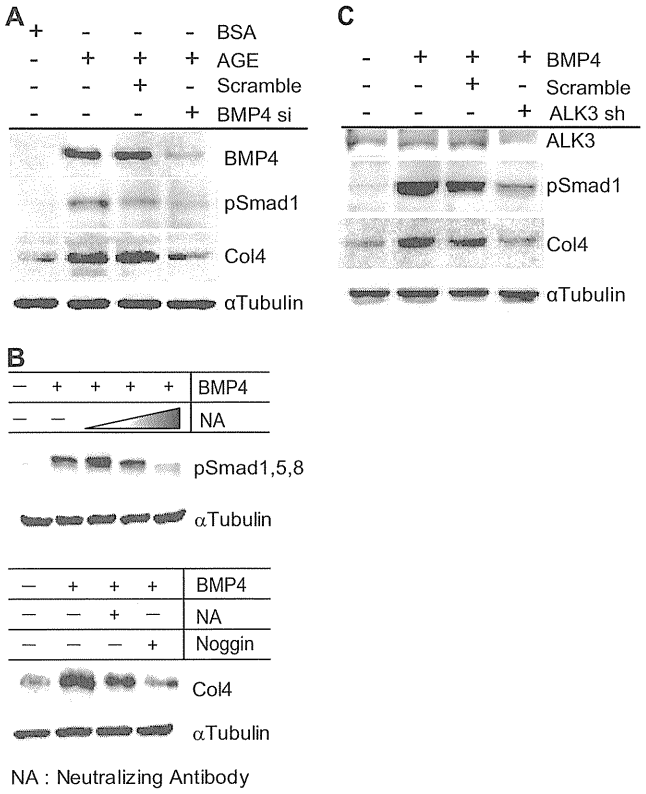

FIGURE 2. **Modulation of Bmp4 signaling.** *A*, expression of Bmp4 and Col4 after treatment with AGE, detected by immunoblot with *Bmp4* siRNA (*siBmp4*) or scrambled siRNA (scramble) for 48 h. *B*, phosphorylation of Smad1/5/8 and expressions of Col4 after stimulation by Bmp4 (20 ng/ml) detected by immunoblot with and without Bmp4-neutralizing antibody or Noggin. *C*, phosphorylation of Smad1/5/8 and expressions of Col4 after stimulation by Bmp4 (20 ng/ml) detected by immunoblot with shRNA for *Alk3* (*shALK3*) or control vector. The data are representative of three independent experiments.

ies. The immunoreactivity of Bmp4 was quantified by Bmp4-positive areas in the glomeruli using image processor for analytical pathology. Tissue for electron microscopy was fixed in 2.5% glutaraldehyde. The mean GBM thickness was calculated with Image J (National Institutes of Health).

RESULTS

Bmp4 Up-regulates Smad1-Col4 Expression through Activation of the AGE-RAGE Signaling Pathway—We previously demonstrated that Smad1 is induced by AGE stimulation in mouse mesangial cells (MCs). Therefore, we first determined the expression of Bmp4 in mouse MCs treated with AGE. Expression of Bmp4 and Col4 was increased by AGE stimulation (1 and 10 $\mu g/cm^2$) (Fig. 1*A*). Longer exposure to AGE (48 and 72 h) remarkably up-regulated the expression of Bmp4 as well as those of Smad1 and Col4 (Fig. 1*B*). Knockdown of the RAGE, which is thought to be the main receptor for AGE, attenuated the inductions of Bmp4 and Col4 by AGE (Fig. 1*C*) (23–25). Phosphorylation of Smad1 (pSmad1) was strongly induced by Bmp4, and induction of Col4 by Bmp4 was observed in a time-dependent manner in mouse MCs (Fig. 1, *D* and *E*). Moreover, Bmp4 induced the expression of Smad1 and type 1 collagen (Col1) as well as Col4 in mouse MCs (Fig. 1*F*). Another ligand carboxymethyl lysine for RAGE also induced the expression of Bmp4 in MCs (Fig. 1*G*). These results suggest that Bmp4 is involved in the regulation of Smad1 activation and subsequent production of ECM proteins downstream of the RAGE signaling pathway in MCs.

Bmp4-Alk3 Signal Transduction Pathway Is Important for the Expression of Col4—We next investigated the effects of the inhibition of Bmp4 signaling in the stimulation of AGE. The increased expression of Col4 caused by AGE was significantly inhibited by the knockdown of *Bmp4* (Fig. 2*A*). Similar results were obtained from an inhibition assay using a neutralizing antibody for Bmp4 or Noggin (Fig. 2*B*). Although the neutralizing antibody for Bmp4 clearly inhibited the phosphorylation of Smad1 (Fig. 2*B*), the inhibitory effect for Col4 was partial. Two BMP type I receptors, activin-like kinase 3 and 6 (Alk3 and Alk6), can bind Bmp4 *in vitro* and are also expressed during kidney and urinary tract development (26). We then performed RT-PCR analyses for mouse MCs in the presence or absence of AGE. Expression of *Alk3*, but not *Alk6*, was detected in MCs in both conditions of AGE (data not shown). Therefore, we carried out knockdown of *Alk3* and confirmed the inhibitory effect of phosphorylation of Smad1 (Fig. 2*C*). Expression of Col4 was